AN ABSTRACT OF THE THESIS OF

Dylan Paul Stankus for the degree of Master of Science in Chemical Engineering presented on December 3, 2010.

Title: Interactions between Natural Organic Matter and Gold Nanoparticles Stabilized with Different Organic Capping Agents

Abstract approved:

_____

Jeffrey A. Nason

The adsorption of natural organic matter (NOM) to the surfaces of natural colloids and engineered nanoparticles is known to strongly influence, and in some cases control, their surface properties and aggregation behavior. As a result, the understanding of nanoparticle fate, transport and toxicity in natural systems must include a fundamental framework for predicting such behavior. Using a suite of gold nanoparticles (AuNPs) with different capping agents, the impact of surface functionality, presence of natural organic matter and aqueous chemical composition (pH, ionic strength, and background electrolytes) on the surface charge and colloidal stability of each AuNP type was investigated. Capping agents used in this study were as follows: anionic (citrate and tannic acid), neutral (2,2,2-[mercaptoethoxy(ethoxy)]ethanol and polyvinylpyrrolidone), and cationic (mercaptopentyl(trimethylammonium)). Each AuNP type appeared to adsorb Suwannee River Humic Acid (SRHA) as evidenced by measureable decreases in zeta potential in the presence of 5 mg C L^{-1} SRHA. It was found that 5 mg C L^{-1} SRHA provided a stabilizing effect at low ionic strength and in the presence of only monovalent ions while elevated concentrations of divalent cations lead to enhanced aggregation. The colloidal stability of the NPs in the absence of NOM is a function of capping agent, pH, ionic strength and electrolyte valence. In the presence of NOM at the conditions examined in this study, the capping agent is a less important determinant of stability and the adsorption of NOM is a controlling factor.

© Copyright by Dylan Paul Stankus
December 3, 2010
All Rights Reserved

Interactions between Natural Organic Matter and Gold Nanoparticles Stabilized with Different Organic Capping Agents

by
Dylan Paul Stankus

A THESIS

Submitted to

Oregon State University

In partial fulfillment of
the requirements for the
degree of

Master of Science

Presented December 3, 2010
Commencement June 2011

Master of Science thesis of Dylan Paul Stankus presented on December 3, 2010.

APPROVED:

_____

Major Professor, representing Chemical Engineering

_____

Head of the School of Chemical, Biological, and Environmental Engineering

_____

Dean of the Graduate School

I understand that my thesis will become part of the permanent collection of Oregon State University libraries. My signature below authorizes release of my thesis to any reader upon request.

_____

Dylan Paul Stankus, Author

ACKNOWLEDGEMENTS

I would like to express my appreciation for all those people who made completion of this thesis possible. Funding has been provided by the Air Force Research Laboratory (under agreement number FA8650-05-1-5041) through the Safer Nanomaterials and Nanomanufacturing Initiative (SNNI) in relation to the design of environmentally-benign nanoparticles. Additional thanks go to the School of Chemical, Biological, and Environmental Engineering for supporting me through Teaching Assistantships in the early stages of my graduate education.

I'd like to acknowledge my thesis committee for their guidance, support, and insight throughout my time at OSU. I would like to give special thanks to my advisor, Jeffrey A. Nason for always being supportive and always having confidence in my ability to plan and execute experiments and present results.

This project was made possible through collaboration with the Jim Hutchinson group at University of Oregon who provided the nanoparticles utilized in the study. I would also like to thank Arianne Neigh at Nanocomposix, Inc. for assistance in AuNP selection. Acknowledgement goes to Sujing Xie at the CAMCOR Surface Analytical Facility for assistance with the TEM imaging and Kathy Motter at the IWW collaboratory for total organic carbon analysis of NOM samples.

Finally I would like to thank my friends and family for supporting me through all my endeavors. Very special thanks goes to three professors at the University of South Carolina who introduced me to research and motivated me to pursue graduate study: Mihaly Czako, Laszlo Martin, and Joseph Flora. Thanks y'all.

CONTRIBUTION OF AUTHORS

Jim Hutchinson and Sam Lohse at the University of Oregon contributed to the manuscript in the form of materials, characterization, and advice.

TABLE OF CONTENTS

TABLE OF CONTENTS (Continued)

LIST OF FIGURES

LIST OF FIGURES (Continued)

LIST OF TABLES

Interactions between Natural Organic Matter and Gold Nanoparticles Stabilized with Different Organic Capping Agents

Chapter 1: Introduction

1.1 Background and Motivation

Nanotechnology is the use of materials at an atomic or molecular scale where quantum effects result in unique electrical, optical, magnetic, photoactive and thermal properties. According to the American Society of testing Materials (ASTM), the current definition of a nanomaterial (NM) is a group of atoms having at least one dimension between 1 and 100 nanometers [1]; this length scale is significant due to the increased ratio of surface area to volume which results in high numbers of atoms on the surface as compared to bulk materials [2]. The relatively recent realization of this phenomenon has opened the door to numerous current and potential applications. In 2008, worldwide production of nano-Ag, titanium dioxide, and carbon nanotubes was estimated at 500, 5000, and 350 tons/year, respectively [3]. At current growth rates, the number of consumer products containing nanomaterials is expected to reach approximately 1500 by 2011 [4]. The explosive interest in nanotechnology is alarming when considering the potential adverse effects which may arise from the anthropogenic release of these materials into the environment.

The occurrence of NMs in the environment is not specific to manufactured products but can be attributed to a suite of sources including natural (e.g., volcanic activity), adventitious (e.g., anthropogenic combustion products), and engineered. Particulate analysis of 10,000 year old ice cores has revealed the presence of carbon nanotubes and fullerenes which have been attributed to natural global combustion products [5]. Air monitoring in urban atmospheres has shown nanoparticles of diameters less than 10 nm to account for more than 36% of total particulate matter from both stationary and vehicular combustion sources [6]. Although these background levels of natural and adventitious nanoparticles are of concern, perhaps more compelling is the

production of novel materials and the sheer volumes of engineered nanoparticles manufactured for commercial and industrial applications [3]. Nanoparticles (NPs) may enter the environment intentionally (e.g., use of zero valent iron NPs for remediation) or by accidental release (e.g., release of silver ions after washing socks embedded with silver nanoparticles (Ag-NPs)) [7, 8]. The unique properties that make NPs appealing could lead to unforeseen health and environmental hazards [9]. Once in the environment, organisms will be exposed to nanomaterials. Toxicologists have demonstrated the uptake, accumulation, and toxicity of nanomaterials in organisms exposed to NPs [2]. Additionally, effects on organisms are dependent on nanomaterial physicochemical properties [2]. Because the NP physicochemical properties will be influenced by environmental conditions it is critical to assess environmental behavior of these materials to gain an understanding of the possible implications.

1.2 Problem Statement

The fate and transport of NPs in aquatic systems will be influenced by many processes. Knowledge of NP stability with respect to aggregation is essential for a complete understanding of more complicated processes including deposition, redox, dissolution and biological interactions where aggregation state is a critical factor dictating particle size and available surface area. Natural organic matter (NOM) is known to control surface chemistry and stability of natural colloids and NPs. NPs are tailored to have specific surface properties for specific applications. These properties will also influence their environmental behavior. There is a need to determine the effects of NP surface functionality on their behavior in aquatic systems, including interactions with NOM.

1.3 Significance

The colloidal stability NPs in aquatic systems is governed by NP characteristics and chemical conditions. The environmental compartment NPs are likely to reside in and the resulting conditions and processes the NPs are subject to will be highly dependent on

aggregation state due to its influence on particle mobility. If conditions favor destabilization of NPs, it is likely that they will settle out of the water column and become incorporated into the sediment. Numerous studies have shown the pH, ionic strength, electrolyte valence, and NOM content of an aquatic system to control the surface charge and aggregation state of NPs. The majority of these investigations have only examined the stability of NPs without surface modification. Organic molecules bound to the NP core, known as capping agents, impart stability through electrostatic repulsion, steric stabilization, or a combination of both mechanisms [10]. Capping agents are becoming increasingly more prevalent in NP synthesis as they are used to stabilize the highly reactive NP surfaces against aggregation and dissolution. Surface modifications of NPs with the same core material may result in different environmental fate and impacts. AgNPs with different capping agents have been shown to exhibit vastly different surface charge and aggregation behavior, as compared to bare AgNPs, under a range of aqueous chemical compositions (pH, ionic strength, and electrolyte valence) [11]. Additionally, surface chemistry of NPs may influence their affinity to interact with and adsorb NOM. The investigations presented here go beyond those in the current literature by examining the interactions of NOM and NPs with a consistent core material, but varying organic capping agents. The significance in examining NPs with different surface characteristics is to relate environmental behavior with specific properties of the NPs and aquatic chemical composition (including NOM content and character).

1.4 Objectives

The broad objective of this study is to improve understanding of the role that NOM plays in the environmental fate and transport of surface modified nanoparticles. The scope of the project was narrowed to focus solely on the influence of one representative NOM (Suwannee River humic acid) on the colloidal stability of one nanoparticle size (≈ 10 nm) and core material (gold) with five structurally different capping agents. Specific objectives were to:

1) Determine intrinsic properties of surface functionalized AuNPs in water;

2) Examine adsorption of NOM to different classes of AuNPs;

3) Examine the influence of NOM on the stability of different classes of AuNPs.

1.5 Approach

The stated objectives were accomplished by conducting laboratory investigations utilizing a suite of gold nanoparticles (AuNPs) with different capping agents to examine the impact of surface functionality, presence of NOM, and aqueous chemical composition (pH, ionic strength, and background electrolytes) on the surface charge and colloidal stability of AuNPs. AuNPs were selected as a model system for use in this study due to the ability to obtain particles with a consistent core and well-defined surface chemistry, allowing a systematic investigation of how different surface coatings influence environmental behavior. Furthermore, AuNPs are more stable with respect to redox and dissolution than other classes of nanomaterials such as AgNPs and some metal oxides. Electrophoretic mobility titrations were performed to investigate the intrinsic surface properties of AuNPs. To examine the adsorption of NOM to the AuNPs, the same titrations were repeated in the presence of Suwannee River Humic Acid at 5 mgTOC/L. To gain an understanding of the role NOM plays in the stability of the AuNPs, aggregation studies were performed over a range of aqueous chemical compositions (ionic strength, electrolyte valence, and presence of NOM).

The remainder of this thesis is divided as follows: Chapter 2 contains general background of the colloidal forces governing particle stability and a pertinent literature review related to the interactions of natural organic matter (NOM) with natural colloids and nanomaterials in the environment, physicochemical properties of NPs, and characterization methods applicable for investigating environmental behavior of NPs; Chapter 3 is comprised of a manuscript, “Interactions between Natural Organic Matter and Gold Nanoparticles Stabilized with Different Organic Capping Agents”; and conclusions and recommendations for future work are outlined in Chapter 4.

Chapter 2: Literature Review

2.1 Colloidal stability

The aggregation behavior of NPs in aquatic environments is governed by particle-particle interactions. Most particles in water have a surface charge that is generally negative but is dependent on the material composition. In the solution immediately surrounding the charged particles, there is a relative excess of counter-ions and a relative deficit of co-ions. The differences in these concentrations are eliminated with increasing distance from the charged surface as the concentration of ions approaches that in bulk solution. This phenomenon is known as the electrical double layer (EDL) and is illustrated in Figures 2.1 and 2.2. When two particles approach each other the overlapping of the EDL results in a repulsive force which prevents particles from colliding and aggregating. The EDL is made up of three layers of charge as shown in Figure 2.1. A charged particle surface has a fixed layer of counter ions sorbed to it known as the stern layer (b). Ions in the stern layer are attracted to the surface by electrostatic interactions (i.e., the affinity of opposite charged ions for each other). The diffuse layer (d) is comprised of free ions which move in the fluid under the influence of electric attraction and thermal motion rather than being firmly anchored such as in the stern layer. The shear layer (c) is actually part of diffuse layer. Its external boundary marks the shear plane which separates the mobile fluid from that which remains attached to the surface when the particle is in motion. The electric potential at this plane is measured by electrophoresis and is known as the zeta potential. Zeta potential is often used as an estimation of the magnitude of the surface charge. Electrophoresis simply refers to the motion of suspended particles as influenced by an applied electric field. The velocity of particles is proportional to their surface charge and the applied field strength [12]. The surface charge interactions between colloids are further discussed in the DLVO interactions section.

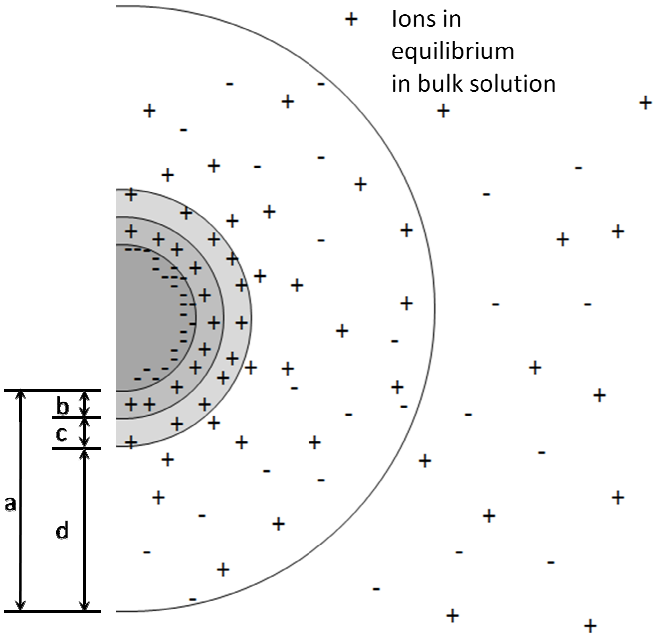

Figure 2.1. Depiction of the electrical double layer surrounding a negatively charged particle surface, where: a.) electrical double layer, b.) fixed charge (stern) layer, c.) shear layer, d.) diffuse ion layer.

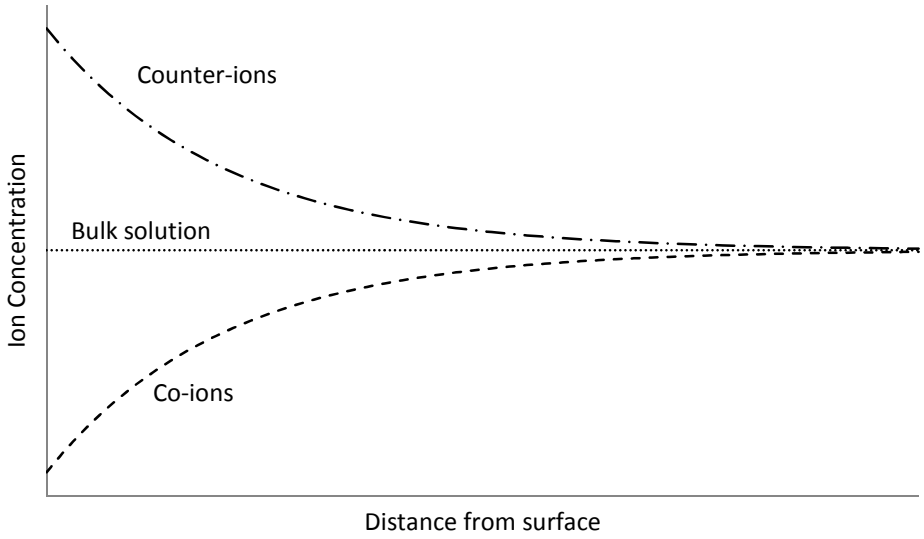

Figure 2.2. Ion concentration as a function of distance from a charged particle surface

Although NPs behave similarly to natural colloids, traditional models used to predict their behavior are not completely applicable and require modification. Interactions between particles in relation to aggregation state are traditionally described by Derjaguin and Landau, Verwey and Overbeek (DLVO) theory but in the case of nanomaterials, non-DLVO forces such as steric, magnetic, and hydration forces can also have an influence [13].

2.1.1 DLVO interactions.

DLVO theory describes aggregation or deposition in terms of the net interaction energy of a particle approaching another particle or surface. The total interaction energy (V_t) that controls colloidal stability of suspended particles is the sum of the repulsive (V_r) and attractive (V_a) forces. Figure 2.3 illustrates the interaction energy of two particles as a function of separation distance. According to traditional DLVO theory, repulsive forces arise from the EDL surrounding particles and the magnitude of this force is proportional to the thickness of the EDL. The thickness of the EDL is a function of particle surface charge and ionic strength. Van der Waals attractive forces result from a varying electromagnetic field due to electrical and magnetic polarizations within the media and in the separation distance between the two surfaces [13]. If particles approach one another with sufficient energy to overcome the resultant net energy barrier from the sum of these forces, as shown in Figure 2.3, aggregation occurs. If aggregation behavior follows DLVO theory, particles will aggregate slowly at low electrolyte concentrations. Under these conditions, a large electrostatic repulsive force causes the rate of aggregation to be controlled by kinetic energy of approaching particles and is referred to as the reaction-limited regime. In this regime, aggregation rate increases with increasing electrolyte concentration. As electrolyte concentration is increased, the rate of aggregation will increase until the energy barrier due to electrostatic repulsion between NPs is eliminated by screening of the surface potential by counter-ions in solution (i.e., compression of the EDL). Figure 2.3 depicts the reduction in repulsive force due to charge screening as the concentration of indifferent ions increases; case (a) representing the lowest ionic strength

and most stable suspension and case (c) an unstable suspension at high ionic strength. Once the energy barrier from electrostatic repulsion is completely eliminated, the rate of aggregation is controlled by Brownian motion of particles and is referred to as the diffusion limited regime. Case (b) in Figure 2.3 represents the electrolyte concentration that signifies the switch from reaction-limited to diffusion-limited aggregation (i.e., the electrolyte concentration where the net energy barrier to aggregation is eliminated) and is known as the critical coagulation concentration (CCC) [12].

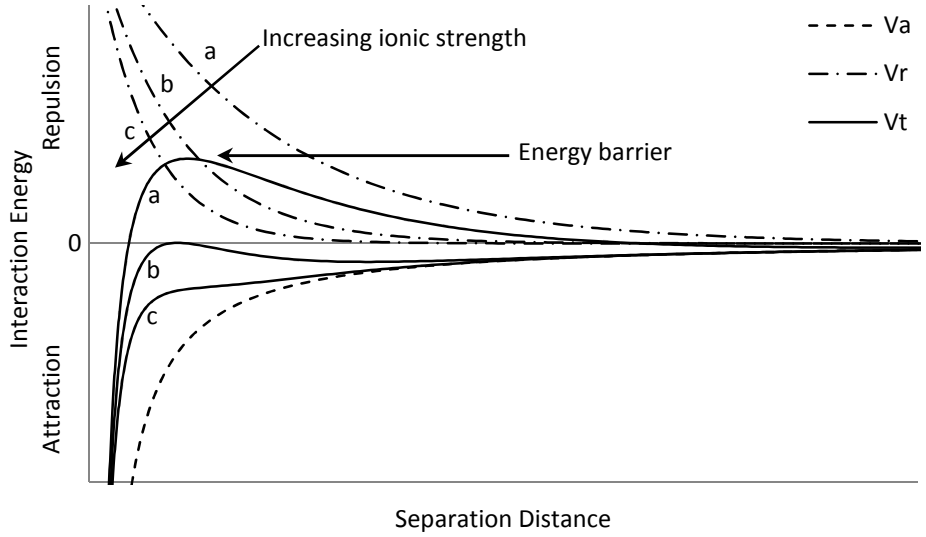

Figure 2.3. Energy of interaction as particles approach one another for (a) a stable, (b) a marginally stable, and (c) an unstable particle suspension. Case (b) represents an ionic strength corresponding to the critical coagulation concentration (CCC).

An understanding of colloidal stability in natural systems is important for engineering applications such as water treatment and contaminant transport. Aggregation of colloids due to compression of the EDL occurs naturally in the environment when mineral or clay particles reach estuaries and the energy barrier is eliminated by high ionic strength. Colloids facilitate surface [14-16] and subsurface [17] contaminant transport when contaminants are sorbed to suspended mineral and clay surfaces. In drinking water treatment it is necessary to remove turbidity from waters in which positive polymeric

substances are utilized to facilitate flocculation and sedimentation of colloids and viruses [12].

2.1.2 Non-DLVO interactions.

A number of forces not described by traditional DLVO theory can influence colloidal stability of suspended particles. Steric repulsive forces result from adsorbed polymers or surfactants used to modify NP surfaces or the adsorption of NOM in aquatic environments and prevent particles from coming into the close contact required for aggregation. When sterically stabilized particles approach each other the interactions between the large chain-like adsorbed molecules cause repulsion due to an increasing number of chain-chain interactions at the expense of more favorable chain-solvent interactions [12]. Hydration forces arise in the case of NPs modified with hydrophilic molecules which may have significant amounts of bound water; an additional repulsive force occurs hindering the approach of the two hydrated surfaces as those water molecules must be displaced for the particles to come into contact [18]. Magnetic forces between some NPs, such as magnetite (Fe_3O_4), may dominate particle interaction energy and contribute to rapid aggregation [13].

2.2 Natural Organic Matter

Natural organic matter collectively refers to the broken down organic matter from organisms in the environment. This includes a wide range of constituents from small molecules such as acetate, to larger macromolecules like humic substances or proteins, to particulate cell biomass [19]. In natural waters, the majority of organic matter is present as humic substances which are complex mixtures of materials formed by biochemical and chemical reactions during the decay and transformation of plant and microbial remains. Humic substances are primarily composed of three fractions distinguished by their solubility and adsorption behavior; humic acids, fulvic acids, and humins [20]. Humic acids are insoluble under highly acidic conditions and can be separated from fulvic acids by precipitation. In general, humic acids are higher molecular weight compounds and are

more hydrophobic than fulvic acids. Humins are largely insoluble NOM fractions, made up of humic acids with a high content of bound minerals [20]. NOM acts as a natural buffer and plays an important role in the cycling of inorganic minerals in the environment.

Well characterized NOM isolates are available through the International Humic Substances Society (IHSS). IHSS provides standard and reference humic substances from various natural sources for research. The current study utilized an IHSS standard humic acid isolated from the Suwannee River in Georgia. Suwannee River humic acid (SRHA) standard was selected as a model NOM for its availability to researchers worldwide, carefully controlled isolation, extensive characterization, and for comparability due to its wide use throughout the literature.

2.3 Interactions between NOM and natural colloids

It is well established that the natural organic matter content of a system controls the surface chemistry and stability of natural inorganic colloids. Tipping and Higgins observed humic substances (HS) to enhance the colloidal stability of hematite particles at 1-500 mM $CaCl_2$ due to steric repulsive forces imparted by the HS [21]. Gibbs studied salinity induced coagulation of colloids from four natural rivers with and without their natural organic coatings. It was observed that coated particles coagulated significantly slower than those without organic coatings [22]. Jekel investigated the stability of silica and kaolinite particles as influenced by pH, ionic strength (*I*), and three different humic substances. Increasing stability of the particles was observed with increasing adsorption of HS and favorable adsorption occurred with high molecular weight HS [23]. In other work, organic macromolecules were found to stabilize hematite particles in the presence of monovalent electrolytes and enhance aggregation when Ca^{2+} was present [24]. Wilkinson et al. examined the aggregation of inorganic colloids (Al, Si, Fe, and Mn) as influenced by the chemical nature and structure of NOM. It was observed that hydrophilic NOM provided stabilization and chain-like NOM accelerated aggregation [25]. In all the above cases, colloidal stability was observed to be controlled by NOM

content and character. In most studies, it was observed that the hydrophobic and high molecular weight fractions of NOM are most efficient at adsorbing and providing stability to colloids through steric mechanisms. Additionally, colloidal behavior of coated particles often deviates from traditional DLVO theory which only accounts for electrostatic repulsion and Van der Waals attractive forces. Any deviations are usually attributed to the steric forces imparted by the NOM and/or the presence of divalent cations and bridging interactions. The influence of NOM on colloidal stability has been shown to be a function of multiple processes which are likely occurring simultaneously and are dependent on the nature of the NOM and aqueous chemical composition (pH, *I*, and electrolyte valence). Because NOM stabilizes natural colloids, it is conceivable that it will have similar influences on engineered NPs.

2.4 Interactions between NOM and NPs

The environmental fate and transport of NPs in aquatic systems will be a function of physiochemical properties of the particles (e.g., size, shape, core material, surface chemistry) and aqueous chemical composition (e.g., pH, *I*, electrolyte valence, natural organic matter content). Numerous studies have shown the pH, ionic strength, electrolyte valence, and NOM content of an aquatic system to control the surface charge and aggregation state of NPs. In these studies, NOM has been found to influence NP stability and surface chemistry for carbon-based nanomaterials [26-34], metal oxides [35-46], metals [47-51], and quantum dots [52]. Table 2.1 summarizes the laboratory studies examining the effects of NOM on the aggregation of NPs. Several publications have described interactions between NPs as conforming to DLVO type interactions [40, 50, 53, 54] and indicate that these systems deviate from that behavior in the presence of multivalent ions and/or the presence of steric repulsive forces imparted by NOM [50]. According to the literature, the physicochemical properties of NPs and the characteristics of NOM will determine the extent of adsorption and the influence on stability. The majority of these studies utilized Suwannee River humic acid as a NOM surrogate.

Table 2.1. Laboratory Studies on the Effect of NOM on NP Aggregation

nanoparticle type	**solution chemistry and NOM surrogate**	**major findings**
nC_{60}*	90-650 mM NaCl ± 1-5 mg/L HA 4-100 mM $MgCl_2$ ± 1 mg/L HA 2.5-40 mM $CaCl_2$ ± 1 mg/L HA pH 7.5-8.5 Suwannee River humic acid	Aggregation kinetics consistent with DLVO theory with the exception of Ca^{2+} and HA*; HA acts to stabilize particles except when I > 10 mM $CaCl_2$, where intermolecular bridging occurs [27]
SWNTs*	1-100 mM NaCl 0.1-10 mM $CaCl_2$ ± 2.5 mg/L TOC* HA or biomacromolecules pH 6 Suwannee River humic acid	HA and biomacromolecules (BSA*, aliginate, LB*) impart steric repulsion; BSA had the most stabilizing effect and aliginate contributed to larger aggregates in the presence of Ca^{2+}. [33]
MWNTs*	Deionized water µm 1% SDS* model 10-100 mg/L NOM Suwannee River NOM	MWNTs are stable in the presence of NOM and river water; the presence of surfactant increases stability [29]
MWNTs	1-500 mM NaCl ± 5 mg/L HA 0.1-30 mM $CaCl_2$ ± 5 mg/L HA 0.05-30 mM $MgCl_2$ ± 5 mg/L HA pH 3-9 Suwannee River humic acid	MWNT stability is controlled by electrostatic interactions; sorption of HA increases stability due to steric repulsion [32]
Al_2O_3	pH 3-7 HA 5-20 mg/L Aldrich humic acid Amherst peat soil humic acid	Colloidal stability was enhanced with HA at or above the PZC*. Under acidic conditions the peat HA contributed to large aggregates. NOM character has effect on colloidal behavior. [41]
Al_2O_3	0-3 mM Ca^{2+} pH 5, 9 Amherst peat soil humic acid (3 sequential extracts)	Polar, short chain HA coated NPs showed increasing aggregation with Ca^{2+}. Low polar, high molecular weight HA enhanced stability of NPs. [40]
α-Fe_2O_3	10-200 mM NaCl ± HA 1-5 mM $CaCl_2$ ± HA pH 8-9 Suwannee River humic acid	The hematite colloids showed enhanced stability when coated with HA in the presence of NaCl as evidenced by an increase in the CCC. The opposite effect was observed in the case of $CaCl_2$. [43]
FeO	pH 2-6 HA = 0-25 mg/L Suwannee River humic acid	HA was found to stabilize NP suspensions. [36]
FeO	pH 2-12 HA = 10-100 mg/L Suwannee River humic acid	Increases in NP concentration contributes to an increase in aggregation. HA stabilizes NPs and shifts the PZC to lower pH. Dissaggregation was enhanced with increasing HA concentrations. [35]

*Acronyms: nC_{60} (60 atom carbon nanoparticle); SWNTs (single-walled carbon nanotube); MWNTs (multi-walled carbon nanotube); BSA (bovine serum albumin); LB (luria-bertani broth); SDS (sodium dodecyl sulfate); HA (humic acid); FA (fulvic acid); TOC (total organic carbon); PZC (point of zero charge)

Table 2.1 continued. Laboratory Studies on the Effect of NOM on NP Aggregation

nanoparticle type	**solution chemistry and NOM surrogate**	**major findings**
$FeO{\cdot}Fe_2O_3$ (magnetite)	1-100 mM NaCl ± 2-20 mg/L HA pH 3-10 Elliot soil humic acid	HA was found to significantly alter aggregation/deaggregation behavior of NPs even at low concentrations. DLVO theory supported experimental results. [46]
TiO_2	5-100 mM $NaNO_3$ 0.2-5 mg/L FA pH 2-8 Suwannee River fulvic acid	FA was found to generally provide steric stabilization under conditions tested. [39]
ZnO NiO TiO_2 Fe_2O_3 SiO_2	0-16 mM Ca^{2+} ± 0-10 mg/L NOM pH 7.8 Suwannee River NOM	NOM controlled stability of NPs tested with the exception of SiO_2 which had the lowest affinity for adsorption of NOM. [44]
Citrate-Au Acrylate-Au	pH = 1.5-12.5 ± 5mg/L HA Suwannee River humic acid	HA was found to enhance stability of organic stabilized Au-NPs [48]
Ag	1-10 mM $NaNO_3$ 1-10 mM $Ca(NO_3)_2$ ± 10 mg/L FA, HA, PHA pH 5, 8 Suwannee River fulvic acid Suwannee River humic acid Peat humic acid (PHA)	Humic substances were found to stabilize AgNPs except at high concentrations of Ca^{2+} in all cases. [47]
B	50-400 mM NaCl 0.6-10 mM $MgCl_2$ 0.6-10 mM $CaCl_2$ ± 15mgC/L HA ± 4.4 mgC/L Aliginate pH 5.6 Suwannee River humic acid	There addition of HA resulted in stabilization in the case of $CaCl_2$ and $MgCl_2$. Aliginate resulted stabilized NPs in the presence of $MgCl_2$ but resulted in increased attachment efficiencies with $CaCl_2$. [50]

*Acronyms: nC_{60} (60 atom carbon nanoparticle); SWNTs (single-walled carbon nanotube); MWNTs (multi-walled carbon nanotube); BSA (bovine serum albumin); LB (luria-bertani broth); SDS (sodium dodecyl sulfate); HA (humic acid); FA (fulvic acid); TOC (total organic carbon); PZC (point of zero charge)

The majority of these studies have investigated NPs without surface modification. A few recent studies have begun to probe the interactions between capped NPs and NOM. Diegoli *et al.* investigated the effects of SRHA, pH, and ionic strength on Au-NPs with citrate and acrylate capping agents [48]. SRHA was found to enhance stability at extreme pH, which was attributed to the replacement of the capping agents and/or over-

coating coating by SRHA. Pallem *et al.* utilized UV-vis and fluorescence emission spectroscopy to further investigate interactions between AuNP capping agents and humic acid [51]. It was concluded that β-D-glucose stabilized AuNPs were replaced by humic acid molecules while citrate stabilized AuNPs were over-coated. In addition to influencing the aggregation behavior of NPs, coatings of Suwannee River humic or fulvic acid have been shown to reduce the dissolution rate of Ag^+ from AgNPs [55]. The work reviewed indicates that interactions between NOM and NPs in aquatic systems influence surface chemistry and stability and that those interactions will also influence environmental transport and fate. There is a need to correlate environmental behavior with specific properties of NPs and aquatic chemical composition (including NOM) for development of predictive models to assess the environmental impacts of NPs. A library of well-defined NPs with varying surface chemistry is essential to gain an understanding of the relationship between NP physicochemical characteristics and their behavior in environmental systems.

2.5 Gold Nanoparticles

To systematically investigate the interactions between NOM and capped NPs, it is desirable to use NPs that vary in well-defined and controllable ways with respect to their surface functionality. Extensive work has focused on varying the size and surface chemistry of NPs with a gold core. As a result, a wide variety of surface chemistries (capping agents) have been developed and are well understood for the gold system [56]. Due to their unique optical properties, gold nanpoparticles (AuNPs) are increasingly being explored for applications ranging from medical imaging and cancer therapy to electronics and chemical sensing [48, 51]. As a result, gold is on the list of the top 5 nanomaterials being incorporated into consumer products [4]. In addition to the existence of libraries of functionalized AuNPs, there are several other advantages to working with gold as a model system. Interactions with molecules at gold surfaces can be probed using techniques like surface enhanced Raman spectroscopy. Also, AuNPs are stable with respect to redox and dissolution, simplifying the experimental system. For all of these

reasons, AuNPs are a promising model system and were chosen as the platform for this work.

2.6 Quantitative Structure-Activity Relationships

The quantitative correlations of chemical structures with well defined processes such as biological or chemical activity is known as quantitative structure-activity relationships (QSARs). The QSAR ideal is based on an assumption that variance in activity is a result of variances in molecular structure. Understanding contaminants at a molecular level is essential for assessing their environmental behavior. Structure activity relationships provide a means for determining environmental outcomes of contaminants based solely on molecular structure. QSARs provide a valuable tool for modeling environmental contaminant fate and transport. Physical and chemical properties for many emerging contaminants are often unavailable and QSARs allow a predictive assessment of the possible detrimental effects of anthropogenic compounds. Additionally, QSARs aid in the engineering of new molecules by allowing design to be directed at enhancing desired properties while suppressing hazardous ones.

The application of QSARs in the field of nanotechnology (nano-QSARs) has yet to be refined. In a recent review, Leszczinski et al., summarized the major steps required for implementation of nano-QSARs as: (1) development of reproducible ways of representing physicochemical properties of NPs that reliably predict properties and environmental effects; (2) development of a framework for grouping NPs into chemical categories or classes; (3) independent modeling of individual classes of NPs due to the high variability in molecular structure [57]. Development of nano-QSARs will aid in the analysis of environmental risks associated with NPs and provide information for the design of safer NPs. The overarching aim of the current work is towards systematically investigating the relationships between organically stabilized NPs and aqueous chemical compositions to identify key parameters which may be utilized for development of structure-activity relationships.

2.7 Physical and Chemical Properties of NPs

Nanomaterials can be described by their physical and chemical properties. It is necessary to characterize materials under simulated environmental conditions to gain an understanding of their environmental fate, transport, and toxicity. The Organization for Economic Co-operation and Development (OECD) has identified a recommended minimal characterization of NPs that should accompany environmental fate, transport, and toxicity testing. Physical and chemical parameters identified are: particle size and size distribution; aggregation state; shape; chemical composition and crystal structure; surface composition; purity and presence of impurities; surface area; surface chemistry; and surface charge [58]. The current work focuses on the aggregation state and surface characteristics of NPs as influenced by environmental conditions.

2.8 Characterization of NPs

Advanced analytical techniques are required to examine the environmental behavior of engineered NPs. Throughout the literature, combinations of microscopic, spectroscopic and light scattering methodologies have been utilized to describe the physicochemical characteristics of NPs suspended in solutions of various aquatic chemical composition. Techniques utilized in the current study and for future work are summarized here.

2.8.1 Electron Microscopy

Imaging techniques applicable for nano-scale visualization are scanning electron microscopy (SEM), transmission electron microscopy (TEM), and atomic force microscopy (AFM). These techniques are able to produce highly magnified images of nanomaterial surfaces or a bulk sample. They provide a direct means for determining parameters such as size, shape, dispersion, and concentration of nanomaterials.

Scanning electron microscopy. Samples are scanned with a high energy beam of electrons which are reflected and collected as secondary electrons, backscattered electrons and x-rays. The SEM can produce detailed black and white images of a samples

surface structure and morphology [59, 60]. A major limitation in SEM imaging is the substantial sample preparation and removal of particles from their natural environment. Environmental scanning electron microscopy (ESEM) has been used to monitor changes in aggregate structure of SRHA as a function of pH and is ideal for monitoring changes in colloidal structure as a function of hydration state [61]. ESEM is able to overcome some limitations of traditional SEM such as imaging in a vacuum and there is no requirement for staining poorly electron dense materials such as humic substances.

Transmission electron microscopy. A beam of electrons is transmitted through an ultra thin slice of specimen, typically dispersed on a support grid, then magnified and focused by an objective lens. With high resolution transmission electron microscopy (HRTEM), the crystallographic structure of materials can be visualized [59]. TEM is commonly utilized for determination of the size and size distribution of NP samples [62]. A drawback to TEM is that the sample must be imaged in a vacuum and one cannot reliably analyze aggregation state with this technique alone. TEM has also been used to visualize the bridging of fullerene nanoparticles by Suwannee River humic acid and Ca^{2+} ions [27].

Atomic force electron microscopy. The specimen surface is raster scanned with piezoelectric scanners by a cantilever with a sharp tipped probe. This technique is non-destructive to the sample and produces quantitative measurements of surface roughness with high three dimensional spatial resolution [59]. The nature of the AFM makes it better suited at visualizing vertical topography than horizontal resolution which is dependent on the cantilever tip sharpness. Thio et al. utilized AFM to quantitatively determine the adhesive behavior of AuNPs to mica surfaces under environmentally relevant conditions (e.g. pH, *I*, and NOM content) [63].

2.8.2 Spectroscopy

Spectroscopy is generally defined as any measure of a quantity as a function of wavelength, frequency, or energy. It is often used to quantify a chemical species and to identify substances by the spectrum emitted or adsorbed by that species.

Ultraviolet-Visible (UV-vis) spectroscopy. A sample is exposed to a light source such as a Xenon lamp and the intensity of transmitted light is collected as a function of wavelength. The analysis is based on the principle that different species absorb light at different wavelengths. Certain metals scatter optical light elastically due to collective resonance of conductive electrons producing a surface plasmon resonance (SPR). The magnitude, peak wavelength, and spectral bandwidth of the SPR is indicative of particle size, shape, composition, and concentration [59]. UV-vis spectroscopy and TEM have been used to correlate extinction coefficients of AuNPs with their core diameters. A calibration curve was produced allowing determination of AuNP average size and concentration based on the location and intensity of the SPR [64]. This technique has been utilized to monitor aggregation of AuNPs and is applicable to any metal with a SPR [48]. One drawback to using UV-vis for nanoparticle analysis is that only metals with a SPR can be investigated. Additionally, due to the qualitative nature of this technique for monitoring NP aggregation it is best suited for preliminary screening.

Surface enhanced raman spectroscopy (SERS). Every molecular structure scatters light through molecular vibrations in a unique manner and collection of this light produces a Raman spectra. Because the Raman signal is generally low, this technique is not applicable for environmentally relevant concentrations. Although, when an incident laser excites surface plasmons on a metal substrate, enhancements in the Raman Signal as much as 10^{14} can occur for molecules located within 20 nm of the metal surface [65]. Utilization of this phenomenon is known as SERS and has been used to analyze the adsorption mechanisms, surface reactions, and surface orientations of organic molecules onto AgNPs and AuNPs [66, 67].

Fluorescence spectroscopy. Ultraviolet light is used to excite molecules in certain compounds that then emit light at a lower energy. Typically, humic substances are fluorescent in nature making this technique well suited for studying interactions of humic substances with NPs. Pallem et al. utilized fluorescence spectroscopy to examine the adsorption mechanisms of SRHA to gold nanoparticles with two different capping agents [51]. Because fluorescence peaks are dependent on concentration, one must exercise

extreme caution in preparing samples for quenching or enhancement studies due to interactions with NPs or capping agents. While this technique allows one to distinguish whether NOM is interacting with the NP core or the capping agent, it does not permit elucidation of specific mechanistic behavior in adsorption reactions.

X-ray photoelectron spectroscopy (XPS). XPS is a quantitative spectroscopic surface analysis technique used to determine the elemental composition, chemical state, and electronic state of elements up to 10 nm from a surface [59]. XPS has been used to quantify the extent of surface oxidation on multi-walled carbon nanotubes which was later correlated to stability by means of the critical coagulation coefficient (CCC) [68]. XPS provides a promising means by which structural properties may be correlated to environmental mobility of NPs. A limitation for utilization of this technique in probing interaction mechanisms between NOM and capped NPs is that elements must be labeled in order to distinguish for instance between carbon from the capping agent or the NOM.

2.8.3 Light Scattering

The intensity fluctuations of scattered laser light provide rapid and nondestructive determination of hydrodynamic diameter, polydispersivity, and surface charge of particles [69].

Dynamic light scattering (DLS). In the current study a Brookhaven Instruments Corporation (BIC) ZetaPALS was utilized for determination of the particle size analysis with DLS. Within the instrument, a detector is fixed at some angle with respect to the direction of an incident light beam at a fixed distance from a volume of particles. Scattered light from each particle reaches the detector. Since particles are moving around randomly in the liquid the distance that the scattered waves travel to the detector vary as a function of time. The delay times of fluctuations in the scattered intensity are related to the diffusion constants and therefore the particle sizes. Small particles moving rapidly cause faster fluctuations than large particles moving slowly. The delay times of these fluctuations is then determined in a time domain using an autocorrelator. The random motions of the particles give rise to fluctuations in the delay time of the scattered light

intensity. The signal is processed by the autocorrelator forming the auto correlation function ($C(t)$).

$$C(t) = Ae^{-2\Gamma t} + B$$

Where A is an optical constant determined by instrument design, t is time delay, and B is the constant background of the function. As t increases, correlation is lost and the function approaches the term B. Γ is related to the relaxation of fluctuations and is calculated by the equation:

$$\Gamma = Dq^2$$

Where q is calculated from the scattering angle θ, the wavelength of incident laser light λ_o, and the refractive index of the fluid n. D is the translational diffusion coefficient.

$$D = \frac{k_B T}{3\pi\eta(t)d}$$

Where k_B is Boltzmann's constant, T is the temperature, $\eta(t)$ is the viscosity of the liquid, and d is the particle diameter. In summary, a laser is directed at sample and the scattered light collected is correlated to the diffusion rate of the suspended particles which is then used to calculate a particle diameter. DLS provides rapid and simple analysis of particle diameter (d) and aggregation rate. According to Rayleigh scattering the intensity (I) of light scattered by a single small particle from a beam of unpolarized light at wavelength (λ) and intensity (I_o) is given by the equation:

$$I = I_o \frac{\left(1+\cos^2\theta\right)}{2R^2}\left(\frac{2\pi}{\lambda}\right)^4\left(\frac{n-1}{n+2}\right)^2\left(\frac{d}{2}\right)^6$$

Where R is the distance to the particle, n refractive index of the suspending liquid, and θ is the scattering angle (90˚). Because the scattering intensity is proportional to d^6, the measurement is biased towards the largest particles in suspension [70]. DLS has been utilized for determination of aggregation kinetics for numerous NPs under various aqueous chemistries [27, 38, 46, 53, 68]. The major drawback to this technique is that careful preparation must be made to ensure no dust or contamination is in the sample.

Additionally, average hydrodynamic diameters of samples will be biased towards the largest dimension of particles which also limits analysis of polydisperse suspensions.

Phase analysis light scattering (PALS). Charged particles dispersed in a liquid will move with an applied charge. The direction and velocity the particles travel is proportional to the sign and magnitude of the applied charge. The particle velocity (v_s) is related to the applied electric field (E) by the following equation:

$$v_s = \mu_e E$$

Where μ_e is defined as the electrophoretic mobility (EPM). In the current study a Brookhaven Instruments Corporation (BIC) ZetaPALS was utilized for determination of the EPM. Briefly, a laser beam is passed through a sample in a cell exposed to an electric field from two electrodes at a 15˚ scattering angle. The light scattered by the particles is Doppler shifted because of the particles movement. The frequency of light scattered into the detector is Doppler shifted proportional to the velocity of the particles. The EPM is then utilized to calculate the zeta potential according to either the Smoluchowski or Hückel approximation which are applicable according to the product of κa (where κ is the Debye length and a is the particle radius). The Smoluchowski and Hückel approximations are applied to particles with a $\kappa a >> 1$ (large EDL) or $\kappa a << 1$ (small EDL), respectively. In the current study, the product κa ranged from approximately 0.8 to 2, where the Hückel approximation is more appropriate. This technique is widely utilized for examining the surface charge behavior of NPs and can be used to examine changes in surface chemistry upon adsorption of NOM [27, 35, 42].

2.9 Summary

Although progress has been made in determining the environmental behavior of nanomaterials, there is still much work to be done. Systematic and strategic investigations need to be made not only to illustrate a qualitative picture of nanomaterials in aquatic matrices but to begin quantifying behavior based on structural properties of NPs. There is a wide consensus for the need to develop reproducible ways of representing

physicochemical properties of NPs that can reliably predict environmental and ecotoxicological effects [2, 9, 13, 57, 71]. It is critical that predictive models such as QSARs be developed to not only to better assess the environmental implications of NMs but to guide toxicity investigations and the safer design of NMs.

The current study used some of the characterization methods discussed above. Initial investigations to the intrinsic surface charge of the capped AuNPs and the influence of NOM were made by means of PALS for determination of electrophoretic mobility. DLS was utilized to quantify aggregation rates under a range of ionic strengths, electrolyte valence, and presence of NOM. UV-vis and TEM were utilized for verification of particle size, concentrations, and aggregation state. Chapter 3 describes implementation of these techniques in detail.

Chapter 3

Interactions between Natural Organic Matter and Gold Nanoparticles Stabilized with Different Organic Capping Agents

Dylan P. Stankus[†], Samuel E. Lohse[‡], James E. Hutchison[‡], and Jeffrey A. Nason*[,†]

***Accepted to Environmental Science and Technology**
November 16, 2010

[†]School of Chemical, Biological and Environmental Engineering, Oregon State University, 103 Gleeson Hall, Corvallis, OR 97331-2702

[‡]Department of Chemistry and Materials Science Institute, University of Oregon, Eugene, OR 97403

*Corresponding author phone: (541) 737-9911; fax (541) 737-3099; e-mail: jeff.nason@oregonstate.edu.

3.1 Abstract

The adsorption of natural organic matter (NOM) to the surfaces of natural colloids and engineered nanoparticles is known to strongly influence, and in some cases control, their surface properties and aggregation behavior. As a result, the understanding of nanoparticle fate, transport and toxicity in natural systems must include a fundamental framework for predicting such behavior. Using a suite of gold nanoparticles (AuNPs) with different capping agents, the impact of surface functionality, presence of natural organic matter and aqueous chemical composition (pH, ionic strength, and background electrolytes) on the surface charge and colloidal stability of each AuNP type was investigated. Capping agents used in this study were as follows: anionic (citrate and tannic acid), neutral (2,2,2-[mercaptoethoxy(ethoxy)]ethanol and polyvinylpyrrolidone), and cationic (mercaptopentyl(trimethylammonium)). Each AuNP type appeared to adsorb Suwannee River Humic Acid (SRHA) as evidenced by measureable decreases in zeta potential in the presence of 5 mg C L^{-1} SRHA. It was found that 5 mg C L^{-1} SRHA provided a stabilizing effect at low ionic strength and in the presence of only monovalent ions while elevated concentrations of divalent cations lead to enhanced aggregation. The colloidal stability of the NPs in the absence of NOM is a function of capping agent, pH, ionic strength and electrolyte valence. In the presence of NOM at the conditions examined in this study, the capping agent is a less important determinant of stability and the adsorption of NOM is a controlling factor.

3.2 Introduction

The number of nanotechnology-based consumer products currently on the market has increased by nearly 379 % from March 2005 (212) to August 2009 (1015) [1]. As research efforts shift towards production and commercialization of nanoparticles (NP), there is a growing need to fully understand the environmental implications of these materials [2]. The objective of this research is to demonstrate the intricate relationship between the surface functionality of NPs and environmental conditions (e.g., pH, ionic

strength (*I*), electrolyte valence, and natural organic matter (NOM)) and identify key parameters for the development of predictive environmental fate and transport models.

The fate and transport of NPs in aquatic systems will be influenced by many processes. Knowledge of NP stability with respect to aggregation is essential for a complete understanding of more complicated processes including deposition, redox, dissolution and biological interactions where aggregation state is a critical factor dictating particle size and available surface area. Furthermore, because NP transport is heavily influenced by aggregation state, it will also be a primary determinant of which environmental compartment NPs end up in (i.e., which conditions and processes the NPs are subject to). NP stability with respect to aggregation is governed by nanoparticle characteristics and environmental conditions. If conditions favor destabilization of NPs, it is likely that they will settle out of the water column and become incorporated into the sediment. Numerous studies have shown the pH, ionic strength, electrolyte valence, and NOM content of an aquatic system to control the surface charge and aggregation state of NPs. In these studies, NOM has been found to influence NP stability for metal oxides [3-5], metals [6-8], carbon-based NPs [9-11], and quantum dots [12]. The effects of mono- and divalent ions and pH on the stability of fullerene and hematite NPs are observed to follow Derjaguin-Landau-Verwey-Overbeek (DLVO) theory. However, in the presence of NOM and Ca^{2+}, enhanced aggregation is observed due to bridging between the NOM, Ca^{2+}, and the NPs [11, 13]. Additionally, low concentrations of NOM were observed to increase the stability of iron oxide NPs via surface-coating; however, higher concentrations of NOM enhanced aggregation [14]. In both of the above cases, the aggregation mechanism of the NPs was altered in the presence of NOM as represented by Suwannee River Humic Acid (SRHA).

Capping agents are becoming increasingly prevalent in NP synthesis and are primarily used to stabilize the highly reactive NP surfaces to aggregation and dissolution. Organic molecules bound to the NP core impart stability through electrostatic repulsion, steric stabilization, or a combination of both mechanisms [15]. In addition to stabilizing properties, capping agents are also utilized to alter surface chemistry of NPs for specific

applications such as drug delivery and to help control size and shape during NP synthesis [16, 17]. Modifications of surface functionality for NPs with the same core material may result in different environmental outcomes. For example, capped silver nanoparticles (AgNP) are generally more stable than bare AgNPs at the same environmental conditions (pH, ionic strength, and electrolyte valence), with sterically stabilized particles proving to be most resistant to aggregation [18]. Additionally, recent work with citrate stabilized AgNPs has shown coatings of Suwannee River humic or fulvic acid to reduce the rate of Ag^{+} ion release [19].

In the current study, gold nanoparticles (AuNPs) are utilized as a model system to investigate the interactions between SRHA and various capped AuNPs under environmentally relevant conditions. Previous studies have shown SRHA to influence the stability of AuNPs with anionic capping agents. Diegoli *et al.* investigated the effects of SRHA, pH, and ionic strength on Au-NPs with citrate and acrylate capping agents [8]. SRHA was found to enhance stability at extreme pH, which was attributed to the replacement of the capping agents and/or over-coating coating with the SRHA. Pallem *et al.* utilized UV-vis and fluorescence emission spectroscopy to further investigate interactions between AuNP capping agents and humic acid [20]. It was concluded that humic acid molecules substituted β-D-glucose molecules, but overcoated citrate molecules used to stabilized AuNPs..

The interactions between humic substances and NPs is likely a function of NP core material, NP capping agent, NP core - capping agent binding mechanism, and NOM character. Because interactions between NOM and NPs in aquatic systems influence surface chemistry and stability, it is expected that NP fate and transport will also be influenced. It is hypothesized that the intrinsic surface chemistry of the NPs will largely determine their affinity to adsorb NOM and ultimately control environmental fate and mobility.

3.3 Materials and Methods

3.3.1 NP Suspension

Gold nanoparticles with five different stabilizing agents were investigated in this study. Two of the AuNP types, 2,2,2-[mercaptoethoxy(ethoxy)]ethanol (MEEE) and mercaptopentyl(trimethylammonium) (MPTMA) were synthesized using a direct synthesis method, the details of which are reported elsewhere [21]. For these particles, capping agents are bound to the gold core through a thiol bond. The other three AuNP types (citrate (CIT), tannic acid (TAN), and 10 KDa polyvinylpyrrolidone (PVP)) were purchased from NanoComposix, Inc. and capping agents are electrostatically bound to the gold core in a disorganized multilayer. Figure 3.1 depicts the structures of the AuNP capping agents. AuNP core diameters ranged from 5 to 12 nm. Table S1 of supporting information summarizes the properties of the AuNPs, as received in aqueous suspension.

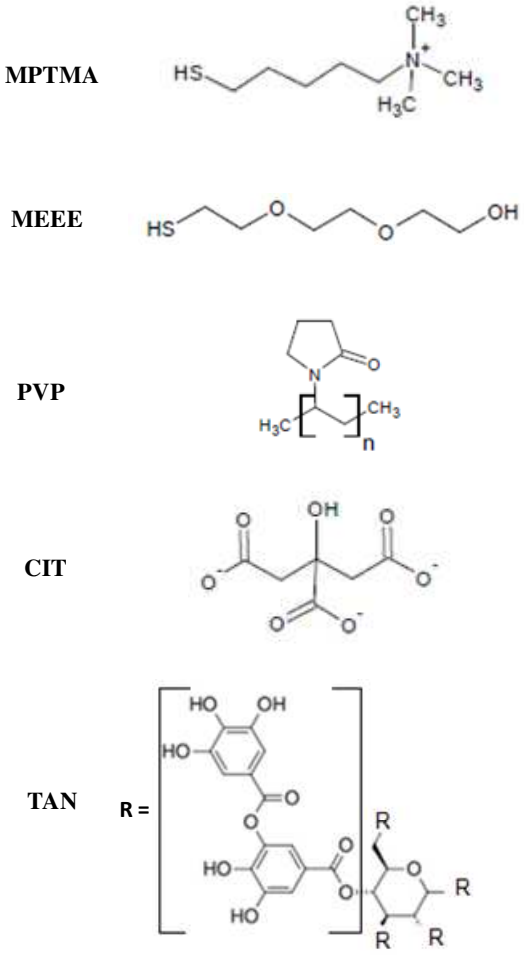

Figure 3.1. Molecular structures of the capping agents used to stabilize gold nanoparticles including mercaptopentyl(trimethylammonium) (MPTMA), 2,2,2-[mercaptoethoxy(ethoxy)]ethanol (MEEE), polyvinylpyrrolidone (PVP), citrate (CIT), and tannic acid (TAN).

3.3.2 Suwannee River Humic Acid Solution

SRHA was purchased from the International Humic Substance Society (IHSS). SRHA was dissolved to a concentration of 40 mg total organic carbon (TOC) L^{-1} at pH 4 as recommended by IHSS. The SRHA solution was allowed to stir for 24 hr in the dark then filtered through a 0.2 µm nylon membrane syringe filter.

3.3.3 Electrolyte Solutions

All inorganic salts used were ACS reagent-grade. Stock solutions, 1 M strength, were prepared for each salt and were filtered through a 0.02 µm syringe filter (Whatman, Anotop 25).

3.3.4 Electrophoretic Mobility Titrations

Electrophoretic mobility titrations were performed with and without SRHA to investigate the influence of NOM on the surface charge of AuNPs. The surface charge was examined as a function of pH (3, 6, 9, and 11, adjusted using 100 mM solutions of KOH or HCl) and as influenced by SRHA (5 mg TOC L^{-1}). NP concentrations were 10 mg L^{-1} as gold. During each electrophoretic mobility measurement, ionic strength (*I)* was held constant at 10 mM by adjusting with KCl as a background electrolyte. A Brookhaven ZetaPALS (Holtsville, NY) was utilized for measurement of electrophoretic mobility and the zeta potential (ζ) was approximated with the Hückel equation [22].

3.3.4 Aggregation Studies

The aggregation state of each AuNP type was studied as a function of ionic strength (10 mM, 50 mM, and 100 mM), electrolyte valence (KCl, $MgCl_2$, and $CaCl_2$), and as influenced by SRHA (5 mg TOC L^{-1}). In all aggregation studies, the ambient pH after dispersion was between 5 and 6 and NP concentrations were 10 mg/L as gold. Samples were prepared in the following sequence: (1) preparation of a 3.5 mL particle-free blank; (2) removal of required volume for Au-NPs, electrolyte, and SRHA; (3) addition of SRHA when applicable; (4) addition of Au-NPs and size verification via

DLS; (5) addition of electrolyte; (6) cuvettes were inverted and immediately analyzed. The aggregation of the AuNP suspensions was quantified using time-resolved dynamic light scattering (TR-DLS) by measuring the intensity-weighted hydrodynamic diameter (D_h) at 15 s intervals for 10 min with a 90Plus particle size analyzer (Brookhaven Instruments, Holtsville, NY). The initial aggregation rate was calculated as the time for an increase of the initial hydrodynamic diameter ($D_{h,0}$) to 1.3*$D_{h,0}$; during this period of time, aggregation is dominated by doublet formation and the rate of change of D_h is proportional to the initial number concentration of primary particle [11]. At later times, the rate of aggregation slows due to the reduction in particle concentration due to aggregation [23]. Figure 3.2 demonstrates the calculation of initial aggregation rate for the MPTMA-AuNPs at I = 100 mM $CaCl_2$. Additional measurements for verification of aggregate size were made by measuring the location and absorbance at the surface plasmon resonance (SPR) peak with UV-vis spectroscopy and with TEM (see Supporting Information).

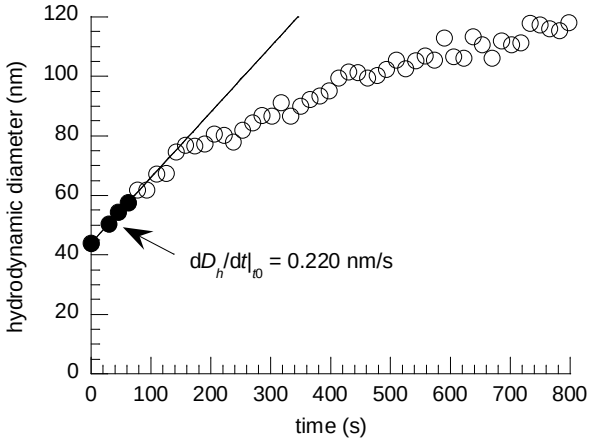

Figure 3.2. Calculation of the initial rate of aggregation from time-resolved dynamic light scattering measurements. Solid spheres indicate data used for the calculation of the slope (D_h <= 1.3$D_{h,0}$). Results shown are for MPTMA-AuNPs at I = 100 mM ($CaCl_2$).

3.4 Results and Discussion

3.4.1 Intrinsic Surface Charge of AuNPs

Electrophoretic mobility titrations were performed on each type of capped AuNP to gain insight into the intrinsic surface charge behavior imparted by each stabilizing agent as a function of pH; these titrations also serve as a basis of comparison for AuNPs suspended in solutions containing SRHA. As expected, each AuNP type exhibited unique behavior. The cationic MPTMA-AuNPs were the only AuNP type to exhibit an isoelectric point (pH≈7.8) between pH 3 and 11 (Figure 3.3a). All other AuNP samples exhibited a negative ζ throughout the pH range tested. The "neutral" AuNPs (PVP and MEEE) had slightly negative ζ ranging from −10 and −15 mV and −15 to −20 mV, respectively (Figure 3.3b, c). Based on electrostatic interactions alone, these particles would be predicted to be moderately stable. Yet, the MEEE- and PVP- AuNPs remained stable over long periods of time (>14 days) at I = 100 mM KCl (see Table 3.1 and associated discussion). Steric repulsion arising from interactions between capping agent molecules bound to the surfaces of adjacent particles (especially, between the large molecular weight PVP molecules) act to stabilize these particles. PVP-AuNPs showed little to no variation in ζ, while the MEEE-AuNPs decreased slightly with increasing pH. This is attributed to an alcohol functional group at the terminal end of the MEEE ligand. The anionic CIT-AuNPs and TAN-AuNPs had slightly more negative ζ of approximately −15 to −25 mV throughout the pH range tested. The CIT-AuNPs remained fairly constant at about −20 mV while the TAN-AuNPs decreased from about −15 to −25 mV with increasing pH. Based on the acid dissociation constants of citrate, one would expect a decreasing trend in ζ with increasing pH, although this was not measured. El Badawy *et al.* demonstrated a decreasing trend in ζ with increasing pH for citrate stabilized silver nanoparticles (CIT-AgNPs) [18].

3.4.2 Interactions between NOM and AuNPs

When electrophoretic mobility titrations were repeated in the presence of 5 mg TOC L^{-1} SRHA, all AuNP types exhibited a decrease in ζ, as shown in Figure 3.3(a-e).

The electrophoretic mobility of SRHA molecules in the absence of NPs was measured and found to be less negative than all of the AuNP+SRHA suspensions (see Supporting Information). On the basis of these results, it appears that SRHA adsorbed to or otherwise interacted with each type of AuNP, regardless of the capping agent. Thus, for each of the AuNP types investigated, the presence of SRHA controls the surface charge, not the initial capping agent functionality. Furthermore, Figure 3.4 shows that for the electrostatically stabilized Au-NPs, ζ was approximately the same for each AuNP type in the presence of SRHA. Initial differences in the surface properties imparted by the capping agents were eliminated in the presence of SRHA, indicating that the organic matter content controls colloid stability, a phenomenon that has been recognized for natural colloids [24] and bare metal oxide nanoparticles [5].

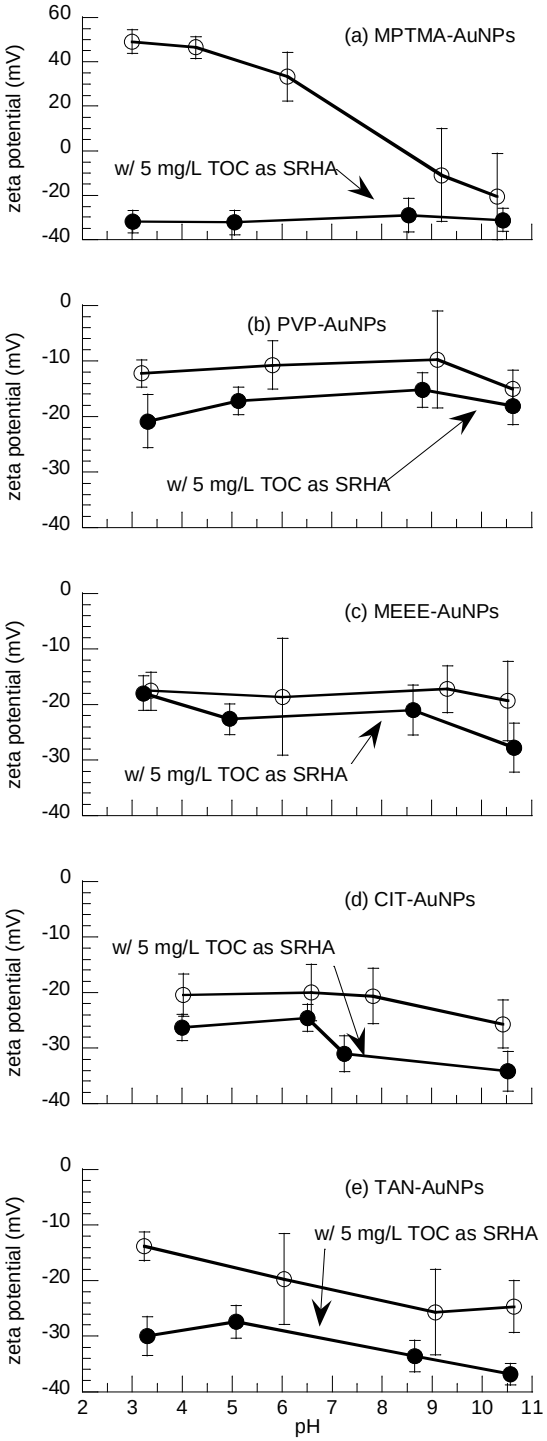

Figure 3.3. The influence of pH and SRHA (5 mg TOC L^{-1}) on the ζ of capped AuNPs at I = 10 mM (KCl) (a) MPTMA-AuNPs, (b) PVP-AuNPs, (c) MEEE-AuNPs, (d) CIT-AuNPs, (e) TAN-AuNPs. Error bars represent 95% confidence intervals.

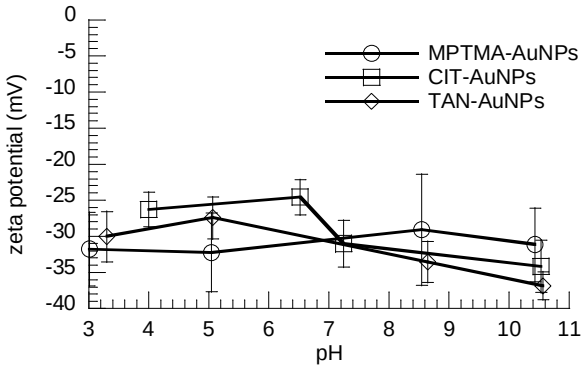

Figure 3.4. Comparison of electrostatically stabilized AuNPs in the presence of 5 mg TOC L^{-1} added as Suwannee River Humic Acid (I = 10 mM as KCl). Error bars represent 95% confidence intervals.

3.4.3 Influence of Ionic Strength and Cation Valence of AuNP Stability

The initial rates of aggregation ($dD_h/dt|_{t0}$) were quantified as a measure of AuNP stability under different conditions of ionic strength and cation valence; these results are summarized in Table 3.2. For the ionic AuNP types (MPTMA, TAN, CIT) in a 1:1 electrolyte (KCl), increasing the ionic strength induced aggregation as evidenced by non-zero values of the initial aggregation rate that increased with increasing ionic strength. These results indicate that electrostatic repulsion between adjacent particle contributed to AuNP stability and that increasing the ionic strength resulted in compression of the electrical double layer, reducing those forces [25]. Because all AuNP types were of approximately the same size and concentration, their relative stability under different conditions can be preliminarily assessed in terms of their relative rates of aggregation. In the presence of a 1:1 electrolyte (KCl), AuNP stability is as follows, PVP ≈ MEEE > MPTMA > TAN > CIT, in order of increasing $dD_h/dt|_{t0}$. The increasing concentrations of KCl did not destabilize the MEEE- and PVP-AuNPs, confirming that steric interactions were also important. When only considering 1:1 electrolytes, NP stability is a function of capping agent size and charge. NPs with neutrally charged, high molecular weight capping agents were the most stable.

Table 3.1. Initial aggregation rate, $dD_h/dt|_{t0}$ (nm/s), as a function of ionic strength and cation valence with and without SRHA (5 mg TOC L^{-1}). The pH of all aggregation samples was between 5 and 6.

AuNP	Ionic Strength (M)								
	KCl			$MgCl_2$			$CaCl_2$		
	0	**0.05**	**0.1**	**0.01**	**0.05**	**0.1**	**0.01**	**0.05**	**0.1**
without SRHA									
MPTMA	0	0.161	0.500	0	0.007	0.273	0	0.005	0.220
PVP	0	0	0	0	0	0	0	0	0
MEEE	0	0	0	0.880	0.692	1.034	0.655	0.789	0.900
CIT	0	0.917	1.233	0.443	0.356	0.449	0.45	0.488	1.053
TAN	0	0.308	1.407	0.780	0.812	0.793	0.824	1.005	1.605
with SRHA (5 mg TOC L^{-1})									
MPTMA	0	0 †	0†	0	0.545*	1.25*	0.019*	1.580*	1.414*
PVP	0	0	0	0	0	0	0	0	0.036*
MEEE	0	0	0	0.488†	1.554*	1.417*	0.542†	1.762*	2.249*
CIT	0	0†	0.275†	0.117†	0.780*	1.292*	0.427†	1.786*	1.668*
TAN	0	0†	0†	1.245*	1.538*	1.275*	0.955*	1.556*	1.825*

† denotes instances where SRHA stabilized AuNPs

* denotes instances where the combination of SRHA and divalent cations resulted in enhanced aggregation.

Several interesting trends were observed when AuNPs were suspended 2:1 electrolytes. The slower rates of aggregation for the MPTMA-AuNPs in $MgCl_2$ and $CaCl_2$ (when compared to KCl) are explained by the fact that the particles were positively charged. At equivalent ionic strengths compared with KCl, Cl^- concentrations (the counter ion in this case) were lower in the 2:1 electrolytes, leading to more diffuse electrical double layers. The sterically stabilized PVP-AuNPs were not influenced by the presence of divalent cations. However, divalent cations did induce aggregation of the

MEEE-AuNPs, CIT-AuNPs, and TAN-AuNPs at I = 10 mM, where the same particles were stable at that ionic strength in the 1:1 electrolyte. With respect to charge screening, divalent cations have a higher charge density and can induce aggregation at lower ionic strength through more efficient double layer compression when compared to monovalent ions [25]. In general, aggregation rates increased with increasing ionic strength in $MgCl_2$ and $CaCl_2$. The fact that some of the initial aggregation rates for CIT- and TAN-AuNPs were lower at similar I between 1:1 and 2:1 electrolytes may be attributed to very fast aggregation occurring in the 15-20 seconds before measurements could be collected.

The presence of Mg^{+2} and Ca^{+2} did induce the aggregation of MEEE-AuNPs where KCl did not, suggesting that mechanisms other than charge screening and steric interactions are also important. In addition to enhanced charge screening by divalent cations, several other effects have been observed in analogous systems. Divalent cation bridging theory (DCB) suggests that non-specific binding occurs between divalent cations and negatively charged functional groups on the surfaces of adjacent molecules. For example, the TAN-AuNPs have relatively large stabilizing ligands with multiple phenolic and carboxylic moieties that could bind with divalent cations. DCB has been shown to accurately describe floc formation in bioreactors through bridging of negatively charged functional groups within the exocellular polymeric substances (EPS) produced by microorganisms by Ca^{2+} and Mg^{2+} [26]. Divalent cations are also known to influence the adsorption and conformation of macromolecules at surfaces and in solution [27]. As such, DCB or other multivalent cation effects cannot be ruled out as a contributing factor for the types of AuNPs examined in this study. In general, the more electropositive cation, Ca^{2+}, was more effective at inducing aggregation than Mg^{2+}. Capping agent functionality, along with ionic strength and cation valence, were the factors controlling AuNP aggregation in the absence of SRHA.

3.4.4 Influence of SRHA on AuNP Stability

The results of the electrophoretic mobility titrations suggest that the presence of SRHA acts to stabilize the AuNPs due in part to the greater electrostatic repulsion

between particles However the adsorption of SRHA is also likely to result in some steric stabilization [11]. In general, this was the case for low ionic strengths and 1:1 electrolyte. Interactions between SRHA and AuNPs provided a stabilizing effect in 1:1 electrolyte solutions as evidenced by the fact that aggregation was induced at higher ionic strengths (Table 3.1). The only AuNP type that aggregated at I = 100 mM KCl was citrate, the least stable AuNP type without SRHA.

At low ionic strengths of the 2:1 electrolytes, SRHA provided a stabilizing effect for MEEE-AuNPs and CIT-AuNPs. However at $I \geq 50$ mM, aggregation was enhanced as evidenced by increased rates of aggregation compared to the trials without SRHA. The increasing rates of aggregation for AuNPs in the presence of SRHA and elevated concentrations of 2:1 electrolytes indicate that interactions between divalent cations and SRHA are important. Recent research has attributed similar behavior in other nanoparticulate systems to DCB [11, 13]. However, the presence of divalent cations can influence several physico-chemical interactions involving humic substances (e.g., cation binding, aggregation, adsorption, and the binding of hydrophobic organic compounds) [27]. Some or all of these processes may be occurring in parallel and are likely influencing one another. The compaction of NOM molecules by cation binding could reduce the steric interactions between NOM coated AuNPs, but this wouldn't explain the dramatic increases in the rates of aggregation between the experiments with and without SRHA. Although not observed directly, DCB appears to be the most plausible explanation for the increased rate of aggregation and large resulting aggregate sizes for AuNPs in the presence of SRHA and elevated concentrations of $CaCl_2$.

MPTMA-AuNPs experienced enhanced aggregation at I = 50 and 100 mM $MgCl_2$, as well as at all ionic strengths tested with $CaCl_2$, which may be an effect of the charge reversal upon the adsorption of SRHA and effects from humic-cation interactions. PVP-AuNPs remained stable in the presence of SRHA with the exception of I = 100 mM $CaCl_2$. Figure 3.5(a-c) illustrates that even the most stable nanoparticle can be destabilized when coated with SRHA in the presence of large concentrations of Ca^{2+}. TAN-AuNPs were observed to have faster aggregation rates in the presence of SRHA

with $MgCl_2$, as compared to KCl, although there was no increasing trend with increasing ionic strength as was the case with $CaCl_2$. The increasing concentration of $CaCl_2$ resulted in increasing initial aggregation rate and aggregate size which is indicative of divalent cation bridging. The specific combinations of ionic strength and cation valence that induced aggregation of AuNPs in this study were for a single SRHA concentration. Different types and concentrations of NOM are likely to result in different behavior and is an area for continued study.

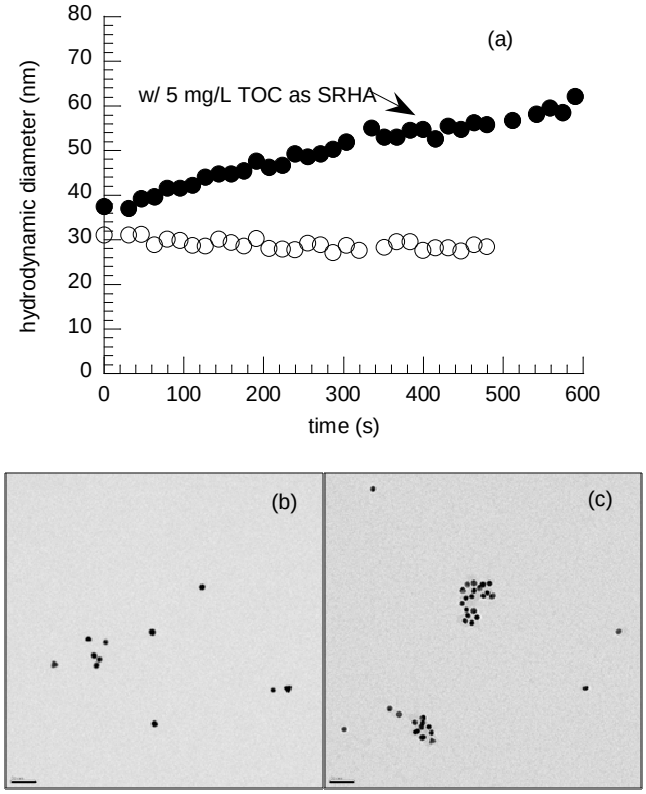

Figure 3.5. The influence of Suwannee River Humic Acid on the aggregation of PVP-AuNPs in the presence of elevated Ca^{+2} (I = 100 mM as $CaCl_2$). (a) time resolved dynamic light scattering results, (b) TEM image of monodisperse particles in the solution without SRHA, (c) TEM image of representative aggregates formed in the solution containing elevated Ca^{+2} and SRHA. Scale bar = 50 nm in the TEM images.

Divalent cation effects (binding and possible bridging) with Mg^{2+} also seem to occur to some extent in the current study. This behavior was not observed in previous work with SRHA and fullerene NPs, possibly due to the low concentration of SRHA (1

mg TOC L^{-1}) [11]. Mg^{2+} has been shown to enhance aggregation of a humic acid extracted from Latahco silt loam at 10 mg TOC L^{-1} by initially binding with anionic groups on the humic acid and gradually forming more stable inner sphere complexes with the humic functional groups [28]. These studies suggest that cation bridging does occur with Mg^{2+}, but that the process is slower and less favorable than with Ca^{2+} due to the larger hydrated radius of Mg^{2+}.

SRHA was found to alter aggregation behavior of all AuNP types and the effects were influenced by ionic strength and electrolyte valence. Aggregation rates did vary between AuNPs with different capping agents in the presence of SRHA, which is likely attributable to different coverage ratios and the nature of the SRHA - AuNP interactions.

3.5 Environmental Implications

As engineers and environmental scientists build models to predict the fate and transport of engineered NPs in the environment, there is a need to relate properties of the NPs with specific environmental behavior. By imparting unique surface chemistry and physico-chemical properties, it would be expected that stabilization through the use of capping agents would strongly influence the processes governing transport, transformation and toxicity. However, results of this work indicate that capping agent functionality may not be the controlling factor for NP mobility in waters with NOM. The presence of SRHA strongly influenced the stability of each type of AuNP tested. In fact, AuNPs with different capping agents had very similar surface properties in the presence of SRHA, suggesting that the NOM content of the system controls particle stability rather than the intrinsic surface chemistry.

As described in the introduction, similar trends have been observed for several other classes of NPs, including metal oxide and carbon-based materials that are more frequently incorporated into consumer products. Nearly universally, it appears that interactions between engineered NPs and NOM have profound implications for NP stability. However, the properties of each NP class will likely play a role in dictating the nature of the NOM-NP interactions. For example, pH may more strongly influence the

adsorption of NOM to an amphoteric metal oxide NP than an AuNP coated with an anionic polymer. Just as toxicologists are aiming to link NP characteristics with toxicity, environmental engineers and scientists should be striving to correlate environmental behavior (e.g., adsorption of NOM and colloidal stability) with those same characteristics. In a recent example of this type of approach, Smith *et al*. [29] correlated multi-walled carbon nanotube stability with surface oxide concentrations.

The influences of aqueous chemical composition on aggregation rates indicate that in aqueous systems without divalent cations, adsorption of NOM will provide enhanced stability, facilitating transport and dispersion. On the other hand, in waters with high divalent cation content, NPs coated with NOM will likely be destabilized, resulting in rapid aggregation and sedimentation. The results from this study are based on a single concentration of a single type of NOM in simple laboratory waters. Such studies are a necessary first step towards understanding the behavior of capped NPs in natural systems. However, these studies should be extended to a wider and more representative range of conditions. By understanding the environmental behavior of NPs, one can make informed decisions on appropriate exposure scenarios and target organisms for toxicity studies. Coupling research efforts focused on environmental fate and distribution with toxicity studies of nanomaterials will enable identification of structural descriptors for the design of safer nanomaterials.

Key parameters for environmental fate and transport models should include stabilizing agent structural descriptors for size, charge, and affinity for NOM adsorption. Quantification of NOM adsorbed in relation to capping agent type could be a good indicator of stability. Continuing work involves performing the same studies with different NOM isolates (e.g. humic and fulvic acids from different sources) and aqueous chemical compositions representative of natural waters to determine if similar effects are observed. Additionally, the mechanisms of NOM adsorption to NP surfaces in relation to capping agent type and connection to the gold core are being investigated.

3.6 Acknowledgements

We thank Arianne Neigh at Nanocomposix, Inc. for assistance with AuNP selection and Sujing Xie at the CAMCOR Surface Analytical Facility for assistance with the TEM imaging. We are grateful to the Oregon State University Research Office and the Air Force Research Laboratory (under agreement number FA8650-05-1-5041) for funding.

3.7 Supporting Information Available

Supporting information includes detailed characterization of the AuNPs used in this study, UV-vis absorbance spectra of the pristine particles, an electrophoretic mobility titration of SRHA without AuNPs, and representative UV-vis, dynamic light scattering and TEM results from aggregation studies.

3.8 References

1. Woodrow Wilson International Center for Scholars. The Project on Emerging Nanotechnologies: Nanotechnology Consumer Product Inventory. 2010 [cited 2010 May, 2010]; Available from: http://www.nanotechproject.org/consumerproducts
2. Erickson, B.E., Nanotechnology Investment. *Chemical & Engineering News*, 2010. **88**(15): p. 22-24.
3. Keller, A.A., et al., Stability and Aggregation of Metal Oxide Nanoparticles in Natural Aqueous Matrices. *Environmental Science & Technology*, 2010. **44**(6): p. 1962-1967.
4. Ghosh, S., et al., Colloidal Stability of Al2O3 Nanoparticles as Affected by Coating of Structurally Different Humic Acids. *Langmuir*, 2010. **26**(2): p. 873-879.
5. Zhang, Y., et al., Impact of natural organic matter and divalent cations on the stability of aqueous nanoparticles. *Water Research*, 2009. **43**(17): p. 4249-4257.
6. Cumberland, S.A. and J.R. Lead, Particle size distributions of silver nanoparticles at environmentally relevant conditions. *Journal of Chromatography A*, 2009. **1216**(52): p. 9099-9105.
7. Johnson, R.L., et al., Natural Organic Matter Enhanced Mobility of Nano Zerovalent Iron. *Environmental Science & Technology*, 2009. **43**(14): p. 5455-5460.
8. Diegoli, S., et al., Interaction between manufactured gold nanoparticles and naturally occurring organic macromolecules. *Science of the Total Environment,* 2008. **402**(1): p. 51-61.

9. Saleh, N.B., L.D. Pfefferle, and M. Elimelech, Influence of Biomacromolecules and Humic Acid on the Aggregation Kinetics of Single-Walled Carbon Nanotubes. *Environmental Science & Technology*, 2010. **44**(7): p. 2412-2418.
10. Lin, D.H., et al., The effect of ionic strength and pH on the stability of tannic acid-facilitated carbon nanotube suspensions. *Carbon*, 2009. **47**(12): p. 2875-2882.
11. Chen, K.L. and M. Elimelech, Influence of humic acid on the aggregation kinetics of fullerene (C-60) nanoparticles in monovalent and divalent electrolyte solutions. *Journal of Colloid and Interface Science*, 2007. **309**(1): p. 126-134.
12. Navarro, D.A.G., et al., Natural Organic Matter-Mediated Phase Transfer of Quantum Dots in the Aquatic Environment. *Environmental Science & Technology*, 2009. **43**(3): p. 677-682.
13. Chen, K.L., S.E. Mylon, and M. Elimelech, Enhanced aggregation of alginate-coated iron oxide (hematite) nanoparticles in the presence of calcium, strontium, and barium cations. *Langmuir*, 2007. **23**(11): p. 5920-5928.
14. Baalousha, M., et al., Aggregation and surface properties of iron oxide nanoparticles: Influence of pH and natural organic matter. *Environmental Toxicology and Chemistry*, 2008. **27**(9): p. 1875-1882.
15. Lead, J.R., Manufactured nanoparticles in the environment Foreword. *Environmental Chemistry*, 2009. **7**(1): p. 1-2.
16. Tolaymat, T.M., et al., An evidence-based environmental perspective of manufactured silver nanoparticle in syntheses and applications: A systematic review and critical appraisal of peer-reviewed scientific papers. *Science of the Total Environment*, 2010. **408**(5): p. 999-1006.
17. Murugadoss, A., A. Khan, and A. Chattopadhyay, Stabilizer specific interaction of gold nanoparticles with a thermosensitive polymer hydrogel. *Journal of Nanoparticle Research*, 2010. **12**(4): p. 1331-1348.
18. El Badawy, A.M., et al., Impact of Environmental Conditions (pH, Ionic Strength, and Electrolyte Type) on the Surface Charge and Aggregation of Silver Nanoparticles Suspensions. *Environmental Science & Technology*, 2010. **44**(4): p. 1260-1266.
19. Liu, J.Y. and R.H. Hurt, Ion Release Kinetics and Particle Persistence in Aqueous Nano-Silver Colloids. *Environmental Science & Technology*, 2010. **44**(6): p. 2169-2175.
20. Pallem, V.L., H.A. Stretz, and M.J.M. Wells, Evaluating Aggregation of Gold Nanoparticles and Humic Substances Using Fluorescence Spectroscopy. *Environmental Science & Technology*, 2009. **43**(19): p. 7531-7535.
21. Lohse, S.E., J.A. Dahl, and J.E. Hutchison, Direct Synthesis of Large Water-Soluble Functionalized Gold Nanoparticles Using Bunte Salts as Ligand Precursors. *Langmuir*, 2010. **26**(10): p. 7504-7511.
22. Hunter, R.J., Zeta potential in colloid science. 1981, New York: Academic Press Inc.

23. Chen, K.L., et al., Assessing the colloidal properties of engineered nanoparticles in water: case studies from fullerene C-60 nanoparticles and carbon nanotubes. *Environmental Chemistry*, 2010. **7**(1): p. 10-27.
24. Tipping, E. and D.C. Higgins, *T*he Effect of Adsorbed Humic Substances on the Colloid Stability of Hematite Particles. *Colloids and Surfaces*, 1982. **5**(2): p. 85-92.
25. Hunter, R.J., ed. Foundations of Colloid Science. Second ed. 2001, Oxford University Press, Inc.: New York, NY.
26. Sobeck, D.C. and M.J. Higgins, Examination of three theories for mechanisms of cation-induced bioflocculation. *Water Research*, 2002. **36**(3): p. 527-538.
27. Tipping, E., Cation binding by humic substances. 1st ed. Cambridge environmental chemistry series. 2002, New York: Cambridge University Press. x, 434 p.
28. Engebretson, R.B. and R. von Wandruszka, Kinetic aspects of cation enhanced aggregation in aqueous humic acids. *Environmental Science & Technology*, 1998. **32**(4): p. 488-493.
29. Smith, B., et al., Influence of Surface Oxides on the Colloidal Stability of Multi-Walled Carbon Nanotubes: A Structure-Property Relationship. Langmuir, 2009. **25**(17): p. 9767-9776.

Chapter 4: Conclusions

Based on the literature reviewed and results from laboratory investigations the following conclusions can be drawn.

- In the absence of SRHA, each AuNP exhibited unique surface charge behavior over the pH range tested as expected. The MPTMA-AuNPs were the only particles to exhibit an isoelectric point at (pH≈7.8). The "neutral" AuNPs (PVP and MEEE) had only slightly negative ζ but remained stable for long periods of time (>14 days) indicating the presence of steric repulsive forces.
- The addition of SRHA resulted in a general trend of decreased ζ for each AuNP. On the basis of this result, it appears that SRHA adsorbed to or otherwise interacted with each AuNP, regardless of capping agent. The presence of SRHA seems to control surface charge for each AuNP, regardless of capping agent. Electrostatically stabilized AuNPs exhibited similar charge behavior as influenced by SRHA, which was quite surprising. Further investigation could reveal that capping agents may be grouped together according to class (e.g. size, charge, etc.).
- Although it was not specifically modeled, aggregation behavior of electrostatically stabilized AuNPs as influenced by monovalent salts appeared to follow DLVO theory. It has been shown consistently throughout the literature that aggregation behavior of natural colloidal particles and NPs in the presence of only monovalent salts and with only electrostatic repulsive forces follow traditional DLVO theory. The stability of PVP- and MEEE- AuNPs in the presence of only monovalent electrolytes in addition to their low surface charge indicated the absence of electrostatic repulsion and the presence of steric repulsive forces.
- The presence of SRHA increased stability of electrostatically stabilized AuNPs in the presence of only monovalent electrolytes. Sorption of NOM resulted in decreased stability in the presence of divalent cations which may be contributed to bridging between SRHA coated particles (a function of divalent content).

Research throughout the literature has attributed similar behavior in other nanoparticle systems to divalent cation bridging [27, 38].

Environmental implications of NPs will be strongly associated to their interactions with NOM in aquatic systems. The influences of aqueous chemical composition on aggregation rates indicate that in aqueous systems without divalent cations, adsorption of NOM will provide enhanced stability, facilitating transport and dispersion. On the other hand, in waters with high divalent cation content, NPs coated with NOM will likely be destabilized, resulting in rapid aggregation and sedimentation.

In general, the results were consistent with literature on colloidal and NP stability. While no modeling was performed, traditional DLVO forces seemed to control stability of NPs with the exception of what appeared to be steric forces imparted by large molecular weight capping agents or NOM and the presence of divalent cations, which is well documented. It seems that traditional models for colloidal stability will need to be modified for coated particles due to their unique properties.

The work presented here goes beyond current knowledge by examining the effects of NP surface functionality on environmental behavior, including interactions with NOM. By imparting unique surface chemistry and physicochemical properties, it was found that stabilization through the use of capping agents strongly influenced the processes governing transport. However, major significance of this work is the indication that capping agent functionality may not be the controlling factor for NP mobility in waters with NOM. The presence of SRHA strongly influenced the stability of each type of AuNP tested. In fact, AuNPs with different capping agents had very similar surface properties in the presence of SRHA, suggesting that the NOM content of the system controls particle stability rather than the intrinsic surface chemistry. This finding demonstrates the need to examine the role of NOM character on the environmental behavior of NPs in addition to intrinsic surface chemistries of NPs. Furthermore, the influences of the NOM isolates on the colloidal stability of AuNPs should be related with NOM composition, as well as the properties of the AuNP capping agents, pH and electrolyte strength and valence.

Future work will be aimed at developing a framework for predicting environmental behavior on the basis of NP characteristics and characteristics of the environmental system to which they are released.

- The physicochemical properties of capping agents will be correlated with interactions between capped NPs in aquatic systems. Using a suite of well-characterized gold nanoparticles (AuNPs) with varying capping agents, stability will be quantified using measurements of the zeta potential and the critical coagulation concentration (CCC) at environmentally relevant pH values in the presence of 1:1 and 2:1 electrolytes. NP stability will then be related to properties of the capping agents (e.g., functionality, ligand length, method of attachment).
- The physicochemical properties of capping agents will be correlated with interactions between capped NPs and natural organic matter surrogates in aquatic systems. It is important to systematically investigate multiple NOM surrogates to gain insight to the role of NOM physicochemical properties (e.g., molecular weight, percent carboxyl functional groups, elemental composition) in interactions with NPs. Measurements of zeta potential and the CCC for capped AuNPs in the presence of various NOM isolates can be used to characterize the influence of NOM on the stability of NPs.
- We also hope to investigate the mechanisms of NOM sorption to capped NPs. Advanced spectroscopic techniques can be used to develop a mechanistic understanding of interactions between natural organic matter and capped NPs. Analysis can be performed on different combinations of NOM, AuNPs, and capping agents to elucidate the mechanisms behind the interactions of NOM with capped NPs.

The additional characterization methods discussed in the literature review provide an avenue to gather the required parameters for predictive models of NM environmental fate and transport. Correlation of physicochemical properties of NMs (shape, size, composition, and surface chemistry) and NOM (molecular weight, elemental

composition, and functionality) with the aggregation behavior of NMs alone and NMs with NOM will lay the groundwork for such models. Combined microscopy techniques can be utilized for characterizing NM size, shape, and polydispersity. Fluorescence spectroscopy, SERS, and XPS can be utilized for qualitative and quantitative analysis of surface functionality, coverage of capping agents and NOM. Quantification of aggregation rates of NMs in aquatic systems is achievable through DLS and the CCC of various NMs can be correlated to surface properties [68]. Determination of surface charge behavior with PALS is another means of investigating and interpreting the influence of capping agents and NOM on NMs. Although these techniques are promising avenues for understanding the environmental implications of NMs, there are still many processes left unaddressed which may lead to deviations from laboratory behavior. Other environmental processes that could significantly affect NM behavior are micro-organisms, natural occurring colloids, biomacromolecules, sunlight, and oxidation/reduction reactions [13].

The proposed research will allow the systematic examination of the interrelated roles of NP capping agents and NOM as drivers for environmental fate and transport. The development of correlations relating environmental behavior with physicochemical properties of NPs and environmental components like NOM will facilitate the continued advancement of predictive models of NP fate and transport currently being developed by researchers in the field. The correlations will also inform the design of safer nanomaterials. A fundamental knowledge of aggregation phenomena provides the foundation for a more complete understanding of NP toxicity and fate in processes like deposition in porous media and redox/dissolution processes where aggregation state is an important factor.

Bibliography

The following sources are referenced in the introduction and literature review portions of this thesis. All other references are noted at the conclusion of the manuscript and the appendices.

1. E2456-06, A.S., Standard Terminology Relating to Nanotechnology. 2010, ASTM International: West Conshohoc, PA.
2. Klaine, S.J., et al., Nanomaterials in the environment: Behavior, fate, bioavailability, and effects. *Environmental Toxicology and Chemistry*, 2008. **27**(9): p. 1825-1851.
3. Mueller, N.C. and B. Nowack, Exposure modeling of engineered nanoparticles in the environment. *Environmental Science & Technology*, 2008. **42**(12): p. 4447-4453.
4. Scholars, W.W.I.C.f. The Project on Emerging Nanotechnologies: Nanotechnology Consumer Product Inventory. 2010 [cited 2010 May, 2010]; Available from: http://www.nanotechproject.org/consumerproducts
5. Murr, L.E., et al., Chemistry and nanoparticulate compositions of a 10,000 year-old ice core melt water. *Water Research*, 2004. **38**(19): p. 4282-4296.
6. Shi, J.P., et al., Sources and concentration of nanoparticles (< 10 nm diameter) in the urban atmosphere. *Atmospheric Environment*, 2001. **35**(7): p. 1193-1202.
7. Benn, T.M. and P. Westerhoff, Nanoparticle silver released into water from commercially available sock fabrics. *Environmental Science & Technology*, 2008. **42**(11): p. 4133-4139.
8. Dickinson, M. and T.B. Scott, The application of zero-valent iron nanoparticles for the remediation of a uranium-contaminated waste effluent. *Journal of Hazardous Materials*, 2010. **178**(1-3): p. 171-179.
9. Maynard, A.D., Safe handling of nanotechnology. *Nature*, 2006. **444**(16).
10. Lead, J.R., Manufactured nanoparticles in the environment Foreword. *Environmental Chemistry*, 2009. **7**(1): p. 1-2.
11. El Badawy, A.M., et al., Impact of Environmental Conditions (pH, Ionic Strength, and Electrolyte Type) on the Surface Charge and Aggregation of Silver Nanoparticles Suspensions. *Environmental Science & Technology*, 2010. **44**(4): p. 1260-1266.
12. Hunter, R.J., ed. Foundations of Colloid Science. Second ed. 2001, Oxford University Press, Inc.: New York, NY.
13. Petosa, A.R., et al., Aggregation and Deposition of Engineered Nanomaterials in Aquatic Environments: Role of Physicochemical Interactions. *Environmental Science & Technology*, 2010. **44**(17): p. 6532-6549.
14. Kimball, B.A., E. Callender, and E.V. Axtmann, Effects of Colloids on Metal Transport in a River Receiving Acid-Mine Drainage, Upper Arkansas River, Colorado, USA. *Applied Geochemistry*, 1995. **10**(3): p. 285-306.

15. Nagorski, S.A. and J.N. Moore, Arsenic mobilization in the hyporheic zone of a contaminated stream. *Water Resources Research*, 1999. **35**(11): p. 3441-3450.
16. Schemel, L.E., B.A. Kimball, and K.E. Bencala, Colloid formation and metal transport through two mixing zones affected by acid mine drainage near Silverton, Colorado. *Applied Geochemistry*, 2000. **15**(7): p. 1003-1018.
17. Ryan, J.N. and M. Elimelech, Colloid mobilization and transport in groundwater. *Colloids and Surfaces a-Physicochemical and Engineering Aspects*, 1996. **107**: p. 1-56.
18. Healy, T.W., et al., Coagulation of Amphoteric Latex Colloids - Reversibility and Specific Ion Effects. *Abstracts of Papers of the American Chemical Society*, 1978. **176**(Sep): p. 113-113.
19. Schwarzenbach, R.P., Gschwend, Philip M., and Imboden, Deiter M., Environmental Organic Chemistry. 2nd ed. 2003, Hoboken, New Jersey: John Wiley and Sons, Inc. 1313.
20. Tipping, E., Cation Binding by Humic Substances. *Cambridge Environmental Chemistry Series*, ed. R.M.H. P.G.C. Cambell, S.J. de Mora. 2002, Cambridge, UK: Cambridge University Press. 434.
21. Tipping, E. and D.C. Higgins, The Effect of Adsorbed Humic Substances on the Colloid Stability of Hematite Particles. *Colloids and Surfaces*, 1982. **5**(2): p. 85-92.
22. Gibbs, R.J., Effect of Natural Organic Coatings on the Coagulation of Particles. *Environmental Science & Technology*, 1983. **17**(4): p. 237-240.
23. Jekel, M.R., The stabilization of dispersed mineral substances by adsoption of humic substances. *Water research*, 1986. **20**(12): p. 1543-1554.
24. O'Melia, C.L.T.a.C.R., Natural organic matter and colloidal stability: models and measurements. *Colloids and Surfaces A: Physicochemical and Engineering Aspects*, 1993. **73**: p. 89-102.
25. Wilkinson, K.J., J.C. Negre, and J. Buffle, Coagulation of colloidal material in surface waters: The role of natural organic matter. *Journal of Contaminant Hydrology*, 1997. **26**(1-4): p. 229-243.
26. Baun, A., et al., Setting the limits for engineered nanoparticles in European surface waters - are current approaches appropriate? *Journal of Environmental Monitoring*, 2009. **11**(10): p. 1774-1781.
27. Chen, K.L. and M. Elimelech, Influence of humic acid on the aggregation kinetics of fullerene (C-60) nanoparticles in monovalent and divalent electrolyte solutions. *Journal of Colloid and Interface Science*, 2007. **309**(1): p. 126-134.
28. Chen, K.L. and M. Elimelech, Interaction of Fullerene (C-60) Nanoparticles with Humic Acid and Alginate Coated Silica Surfaces: Measurements, Mechanisms, and Environmental Implications. *Environmental Science & Technology*, 2008. **42**(20): p. 7607-7614.
29. Hyung, H., et al., Natural organic matter stabilizes carbon nanotubes in the aqueous phase. *Environmental Science & Technology*, 2007. **41**(1): p. 179-184.

30. Hyung, H. and J.H. Kim, Natural organic matter (NOM) adsorption to multi-walled carbon nanotubes: Effect of NOM characteristics and water quality parameters. *Environmental Science & Technology*, 2008. **42**(12): p. 4416-4421.
31. Lin, D.H., et al., The effect of ionic strength and pH on the stability of tannic acid-facilitated carbon nanotube suspensions. *Carbon*, 2009. **47**(12): p. 2875-2882.
32. Saleh, N.B., L.D. Pfefferle, and M. Elimelech, Aggregation Kinetics of Multiwalled Carbon Nanotubes in Aquatic Systems: Measurements and Environmental Implications. *Environmental Science & Technology*, 2008. **42**(21): p. 7963-7969.
33. Saleh, N.B., L.D. Pfefferle, and M. Elimelech, Influence of Biomacromolecules and Humic Acid on the Aggregation Kinetics of Single-Walled Carbon Nanotubes. *Environmental Science & Technology*, 2010. **44**(7): p. 2412-2418.
34. Xie, B., et al., Impact of natural organic matter on the physicochemical properties of aqueous C-60 nanoparticles. *Environmental Science & Technology*, 2008. **42**(8): p. 2853-2859.
35. Baalousha, M., Aggregation and disaggregation of iron oxide nanoparticles: Influence of particle concentration, pH and natural organic matter. *Science of the Total Environment*, 2009. **407**(6): p. 2093-2101.
36. Baalousha, M., et al., Aggregation and surface properties of iron oxide nanoparticles: Influence of pH and natural organic matter. *Environmental Toxicology and Chemistry*, 2008. **27**(9): p. 1875-1882.
37. Chen, K.L., S.E. Mylon, and M. Elimelech, Aggregation kinetics of alginate-coated hematite nanoparticles in monovalent and divalent electrolytes. *Environmental Science & Technology*, 2006. **40**(5): p. 1516-1523.
38. Chen, K.L., S.E. Mylon, and M. Elimelech, Enhanced aggregation of alginate-coated iron oxide (hematite) nanoparticles in the presence of calcium, strontium, and barium cations. *Langmuir*, 2007. **23**(11): p. 5920-5928.
39. Domingos, R.F., N. Tufenkji, and K.J. Wilkinson, Aggregation of Titanium Dioxide Nanoparticles: Role of a Fulvic Acid. *Environmental Science & Technology*, 2009. **43**(5): p. 1282-1286.
40. Ghosh, S., et al., Colloidal Stability of Al2O3 Nanoparticles as Affected by Coating of Structurally Different Humic Acids. *Langmuir*, 2010. **26**(2): p. 873-879.
41. Ghosh, S., et al., Colloidal Behavior of Aluminum Oxide Nanoparticles As Affected by pH and Natural Organic Matter. *Langmuir*, 2008. **24**(21): p. 12385-12391.
42. Keller, A.A., et al., Stability and Aggregation of Metal Oxide Nanoparticles in Natural Aqueous Matrices. *Environmental Science & Technology*, 2010. **44**(6): p. 1962-1967.
43. Mylon, S.E., K.L. Chen, and M. Elimelech, Influence of natural organic matter and ionic composition on the kinetics and structure of hematite colloid

aggregation: Implications to iron depletion in estuaries. *Langmuir*, 2004. **20**(21): p. 9000-9006.
44. Zhang, Y., et al., Impact of natural organic matter and divalent cations on the stability of aqueous nanoparticles. *Water Research*, 2009. **43**(17): p. 4249-4257.
45. Zhang, Y., et al., Stability of commercial metal oxide nanoparticles in water. *Water Research*, 2008. **42**(8-9): p. 2204-2212.
46. Hu, J.D., et al., Effect of dissolved organic matter on the stability of magnetite nanoparticles under different pH and ionic strength conditions. *Science of the Total Environment,* 2010. **408**(16): p. 3477-3489.
47. Cumberland, S.A. and J.R. Lead, Particle size distributions of silver nanoparticles at environmentally relevant conditions. *Journal of Chromatography A*, 2009. **1216**(52): p. 9099-9105.
48. Diegoli, S., et al., Interaction between manufactured gold nanoparticles and naturally occurring organic macromolecules. *Science of the Total Environment*, 2008. **402**(1): p. 51-61.
49. Johnson, R.L., et al., Natural Organic Matter Enhanced Mobility of Nano Zerovalent Iron. *Environmental Science & Technology*, 2009. **43**(14): p. 5455-5460.
50. Liu, X.Y., et al., Effects of natural organic matter on aggregation kinetics of boron nanoparticles in monovalent and divalent electrolytes. *Journal of Colloid and Interface Science*, 2010. **348**(1): p. 101-107.
51. Pallem, V.L., H.A. Stretz, and M.J.M. Wells, Evaluating Aggregation of Gold Nanoparticles and Humic Substances Using Fluorescence Spectroscopy. *Environmental Science & Technology*, 2009. **43**(19): p. 7531-7535.
52. Navarro, D.A.G., et al., Natural Organic Matter-Mediated Phase Transfer of Quantum Dots in the Aquatic Environment. *Environmental Science & Technology*, 2009. **43**(3): p. 677-682.
53. Buettner, K.M., C.I. Rinciog, and S.E. Mylon, Aggregation kinetics of cerium oxide nanoparticles in monovalent and divalent electrolytes. *Colloids and Surfaces a-Physicochemical and Engineering Aspects*, 2010. **366**(1-3): p. 74-79.
54. Mulvihill, M.J., et al., Influence of Size, Shape, and Surface Coating on the Stability of Aqueous Suspensions of CdSe Nanoparticles. *Chemistry of Materials*, 2010. **22**(18): p. 5251-5257.
55. Liu, J.Y. and R.H. Hurt, Ion Release Kinetics and Particle Persistence in Aqueous Nano-Silver Colloids. *Environmental Science & Technology*, 2010. **44**(6): p. 2169-2175.
56. Woehrle, G.H., L.O. Brown, and J.E. Hutchison, Thiol-functionalized, 1.5-nm gold nanoparticles through ligand exchange reactions: Scope and mechanism of ligand exchange. *Journal of the American Chemical Society*, 2005. **127**(7): p. 2172-2183.
57. Tamasz Puzyn, D.L., and Jerzy Laszczynski, Toward the development of "Nano-QSARs": Advances and Challenges. Small, 2009. **5**(22): p. 2494-2509.

58. OECD, Guidance manual for the testing of manufactured nanomaterials: OECD's sponsorship Programme; First Revision, in *OECD Environment, Health and Saftey Publications on the safety of Manufactured Nanomaterials*. 2009, OECD: Paris.
59. M Joshi, A.B., and S Wazed Ali, Characterization techniques for nanotechnology applications in textiles. *Indian Journal of Fibre & Textile Research*, 2008. **33**: p. 304-317.
60. Singh, A.K., V. Viswanath, and V.C. Janu, Synthesis, effect of capping agents, structural, optical and photoluminescence properties of ZnO nanoparticles. *Journal of Luminescence*, 2009. **129**(8): p. 874-878.
61. Redwood, P.S., et al., Characterization of humic substances by environmental scanning electron microscopy. *Environmental Science & Technology*, 2005. **39**(7): p. 1962-1966.
62. Balan, L., et al., Silver nanoparticles: New synthesis, characterization and photophysical properties. *Materials Chemistry and Physics*, 2007. **104**(2-3): p. 417-421.
63. Thio, B.J.R., et al., Measuring the Influence of Solution Chemistry on the Adhesion of Au Nanoparticles to Mica Using Colloid Probe Atomic Force Microscopy. *Langmuir*, 2010. **26**(17): p. 13995-14003.
64. Liu, X.O., et al., Extinction coefficient of gold nanoparticles with different sizes and different capping ligands. *Colloids and Surfaces B-Biointerfaces*, 2007. **58**(1): p. 3-7.
65. Halvorson, R.A. and P.J. Vikesland, Surface-Enhanced Raman Spectroscopy (SERS) for Environmental Analyses. *Environmental Science & Technology*, 2010. **44**(20): p. 7749-7755.
66. Bae, S.J., et al., Adsorption of 4-biphenylisocyanide on gold and silver nanoparticle surfaces: Surface-enhanced Raman scattering study. *Journal of Physical Chemistry B*, 2002. **106**(28): p. 7076-7080.
67. Lee, C.R., et al., Surface-enhanced Raman scattering of 4,4 '-dicyanobiphenyl on gold and silver nanoparticle surfaces. *Journal of Raman Spectroscopy*, 2002. **33**(6): p. 429-433.
68. Smith, B., et al., Influence of Surface Oxides on the Colloidal Stability of Multi-Walled Carbon Nanotubes: A Structure-Property Relationship. *Langmuir*, 2009. **25**(17): p. 9767-9776.
69. Sattelle, D.B., Quasielastic Laser-Light Scattering and Laser Doppler Electrophoresis as Probes of Synaptic and Secretory Terminal Function. *Journal of Experimental Biology*, 1988. **139**: p. 233-252.
70. Hassellov, M., et al., Nanoparticle analysis and characterization methodologies in environmental risk assessment of engineered nanoparticles. *Ecotoxicology*, 2008. **17**(5): p. 344-361.
71. Depledge M.H., P.L.J., and J.H. Lawton, Nanomaterials and the Environment: The Views of the Royal Commission on Environmental Pollution (UK). *Environmental Toxicology and Chemistry*, 2010. **29**(1): p. 1-4.

Appendix A: Supporting Information

Ligand-stabilized Gold Nanoparticles

The diameter of the pristine AuNPs was determined by dynamic light scattering (DLS) (Brookhaven 90plus) and transmission electron microscopy (TEM) (FEI Titan 80 - 300). The intensity weighted hydrodynamic diameter (D_h) of the AuNPs is larger than the diameter determined from TEM because D_h includes the ligand shell. Based on the differences between DLS and TEM sizes, it is clear that the particles had ligands attached to the surface. UV-Vis spectroscopy was utilized to measure the presence of a Surface Plasmon Resonance (SPR) peak as an additional verification of size and to determine the concentration of the AuNP suspensions [1]. All measurements were performed at a nanoparticle concentration of 10 mg L^{-1} as gold atoms. The zeta potential and pH reflect the surface charge of the AuNPs, suspended in distilled deionized water. Characteristics of the pristine AuNPs, as received, are shown in Table A1. TEM images of the particles are shown in Figure A1. UV-vis spectra are shown in Figure A2.

Table A1. Characteristics of capped gold nanoparticles as received and dispersed in distilled deionized water.

AuNP	TEM size (nm)	D_h[a] (nm)	SPR peak wavelength (nm)	total Au concentration[b] (mg L^{-1})	ζ potential (mV)	pH	stabilization mechanism
MPTMA	10	26.4 ± 0.2	517	172.1	+ 7.7	7.4	electrosteric
PVP	11.4	28.3 ± 1.4	525	3381.6	− 4.2	5.8	steric
MEEE	5.7	30.9 ± 1.0	516	106.1	− 9.3	6.4	steric
CIT	11.3	24.9 ± 3.6	519	200	− 32.5	6.6	electrostatic
TAN	12.5	27.2 ± 0.8	526	2038.8	− 46.5	6.0	electrosteric

[a] Hydrodynamic diameter ± 95% confidence interval
[b] Concentration determined by UV-vis spectroscopy [1]

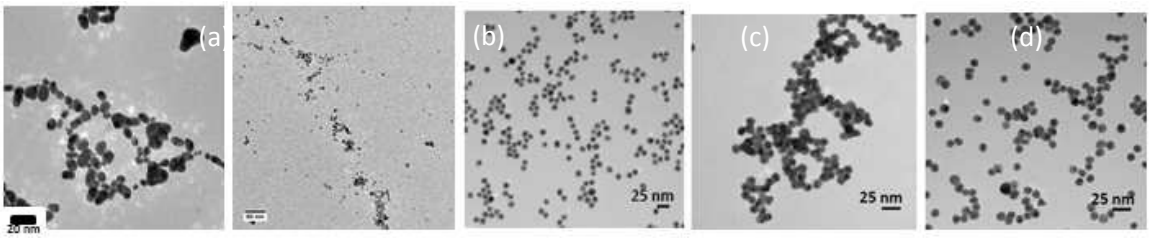

Figure A1. TEM images for the AuNPs as received a) MPTMA-AuNPs b) MEEE-AuNPs c) PVP-AuNPs d) CIT-AuNPs e) TAN-AuNPs

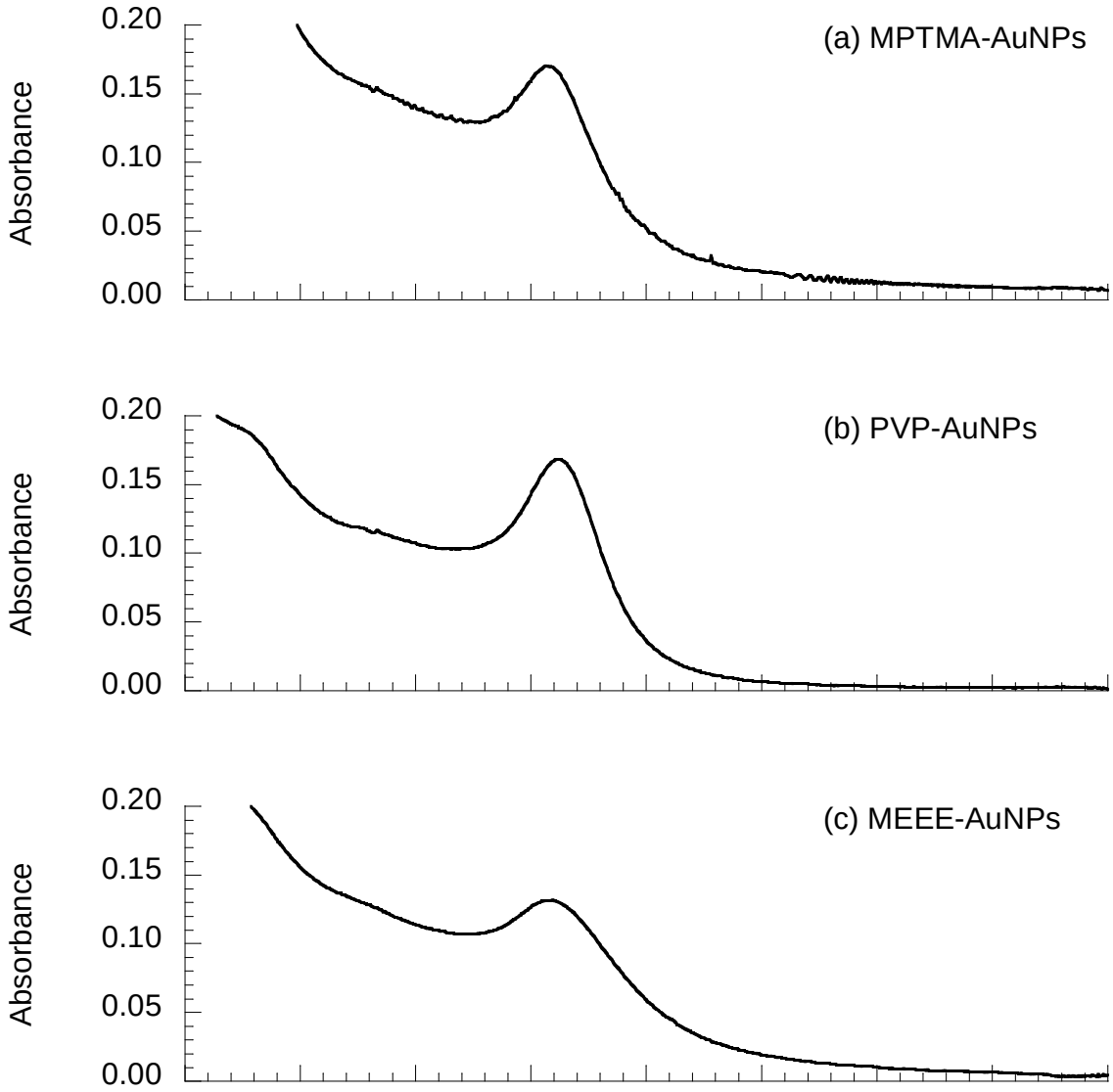

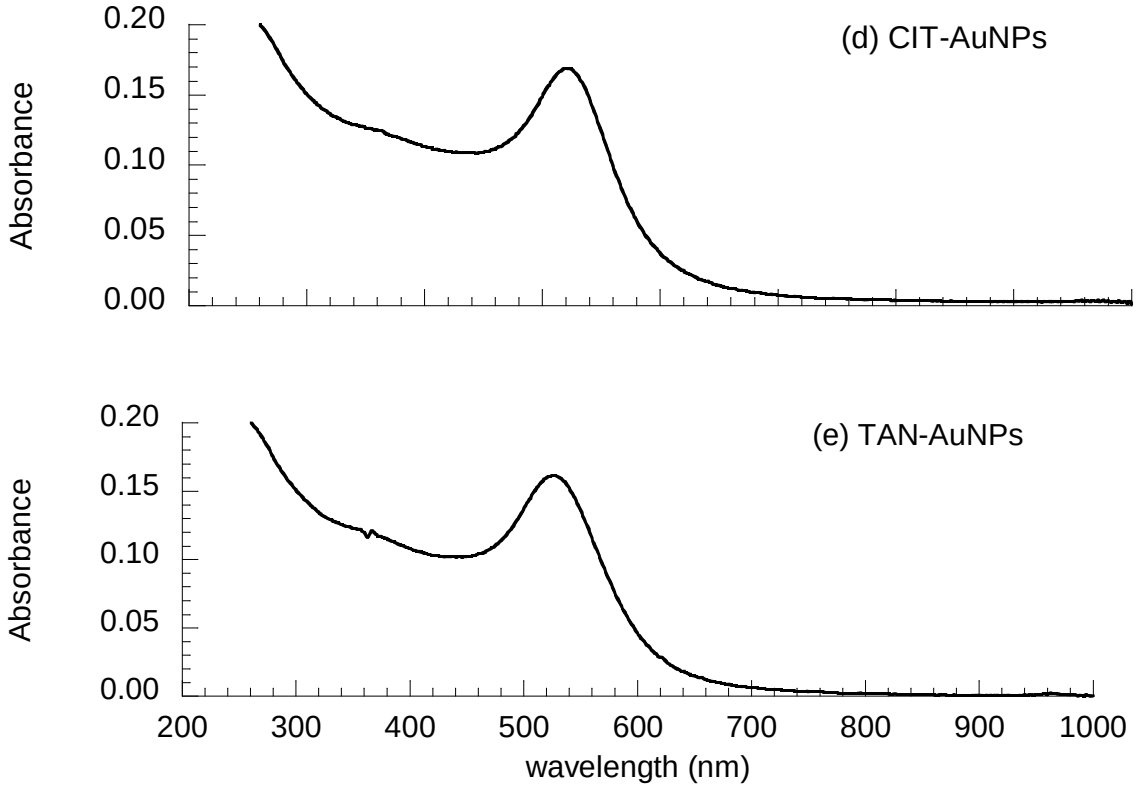

Figure A2. UV-vis absorbance spectra of ligand-stabilized AuNPs in distilled deionized water (a) MPTMA-AuNPs, (b) PVP-AuNPs, (c) MEEE-AuNPs, (d) CIT-AuNPs, (e) TAN-AuNPs. Particle size and concentration were estimated from the characteristics of the surface plasmon resonance peak following the procedure outlined by Liu *et al*. [1] and results are shown in Table S1.

Zeta potential of Suwannee River Humic Acid

The electrophoretic mobility of SRHA was measured in 10 mM KCl at pH 5.5 without AuNPs and zeta potentials were estimated using the Hückel Equation.

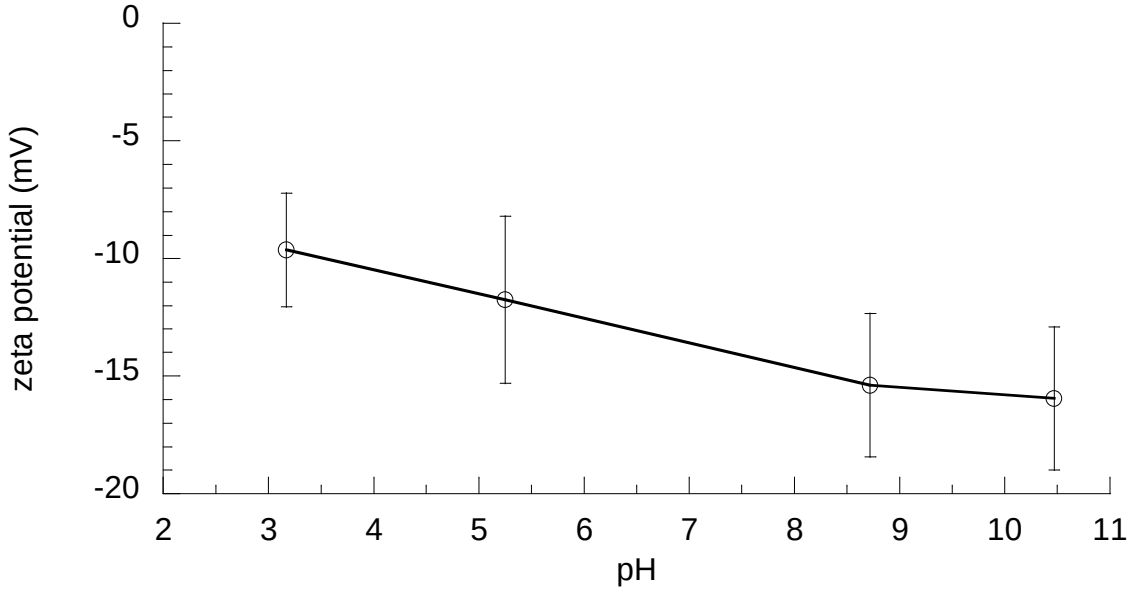

Figure A3. The influence of pH on the zeta potential of Suwannee River Humic Acid in 10 mM KCl.

Representative results from aggregation studies

Three methods were used to verify the results of the aggregation studies. First, preliminary screens using UV-vis spectroscopy were performed, followed by time-resolved dynamic light scattering experiments. Finally, suspensions from the dynamic light scattering experiments were examined by transmission electron microscopy. Complete results from a single set of experiments involving CIT-AuNPs in I = 50 mM (KCl) with and without 5 mg L^{-1} TOC (as SRHA) are displayed in Figures A4-A6.

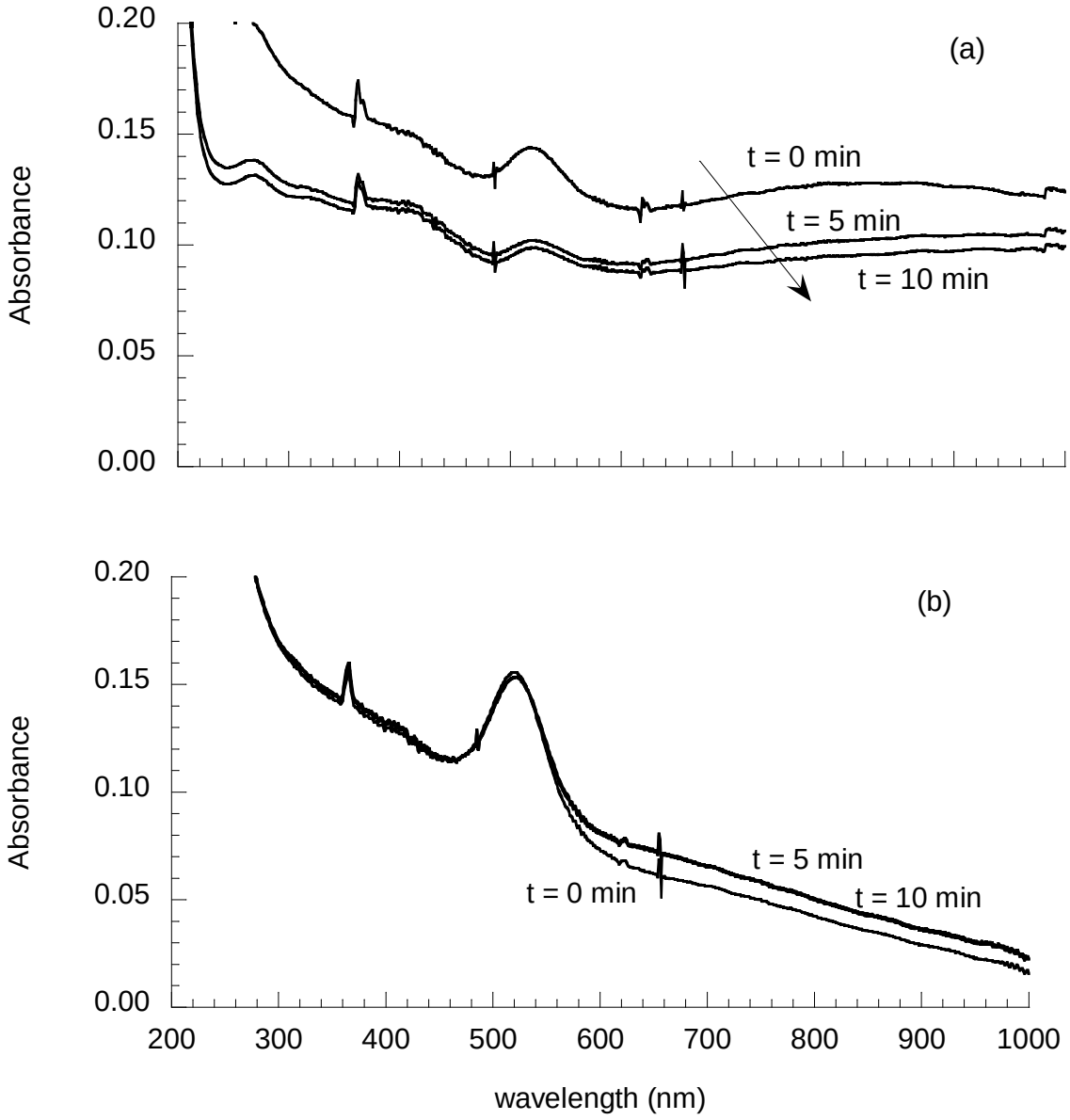

Figure A4. UV-vis scans of CIT-AuNPs in I = 50 mM (KCl) solution (a) without SRHA, (b) with 5 mg L^{-1} TOC (SRHA). Reduction and broadening of the surface plasmon resonance peak indicate aggregation of the particles [2]. Clearly, the presence of SRHA stabilizes the CIT-AuNPs at this ionic strength of a 1:1 electrolyte.

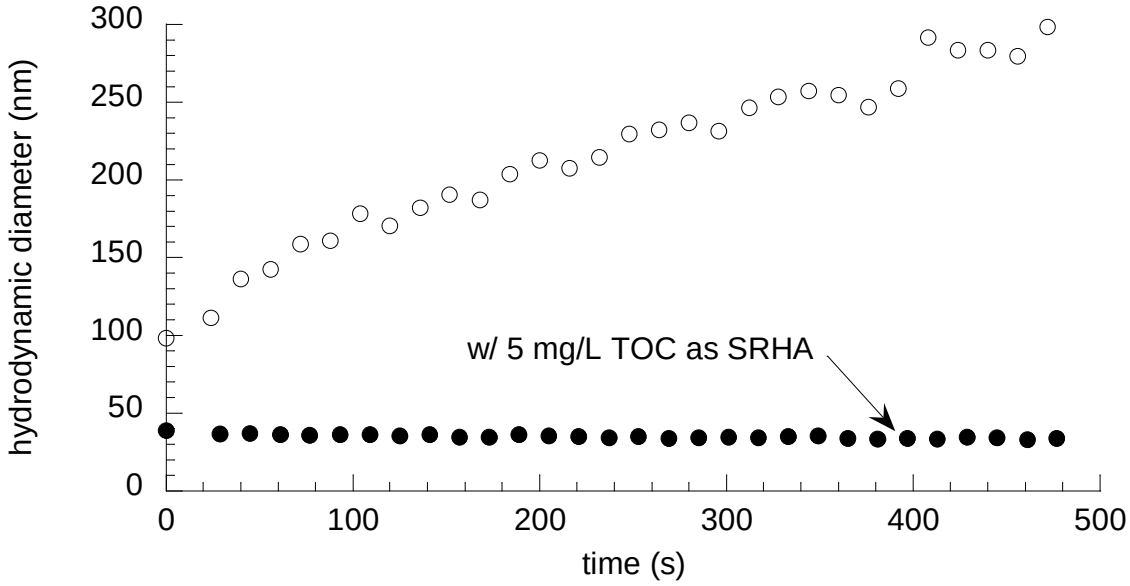

Figure A5. Time-resolved dynamic light scattering results from CIT-AuNPs suspended in I = 50 mM (KCl) with and without 5 mg L^{-1} TOC (SRHA). Rapid aggregation occurred when NPs were added to the electrolyte alone, however no aggregation was seen in the solution containing SRHA.

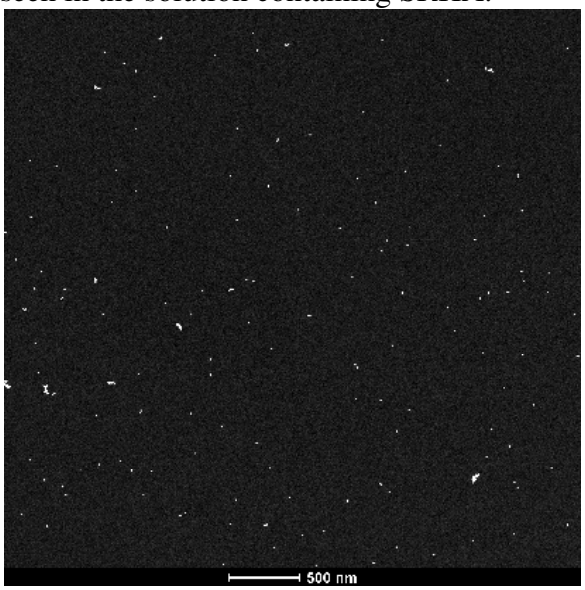

Figure A6. TEM image of CIT-AuNPs that had been suspended in I = 50 mM (KCl) with 5 mg L^{-1} TOC (SRHA) for approximately 1 hr prior to deposition on the TEM grid. Although some aggregates can be seen, the majority of the NPs remained dispersed, confirming the results from the UV-vis and DLS measurements.

Additional Data on Divalent Cation Effects

Results from time-resolved dynamic light scattering experiments involving CIT-AuNPs in the presence of varying concentrations of calcium and SRHA are shown in Figure A7. This is the raw data used to generate the initial aggregation rates presented in Table 1 of the main text.

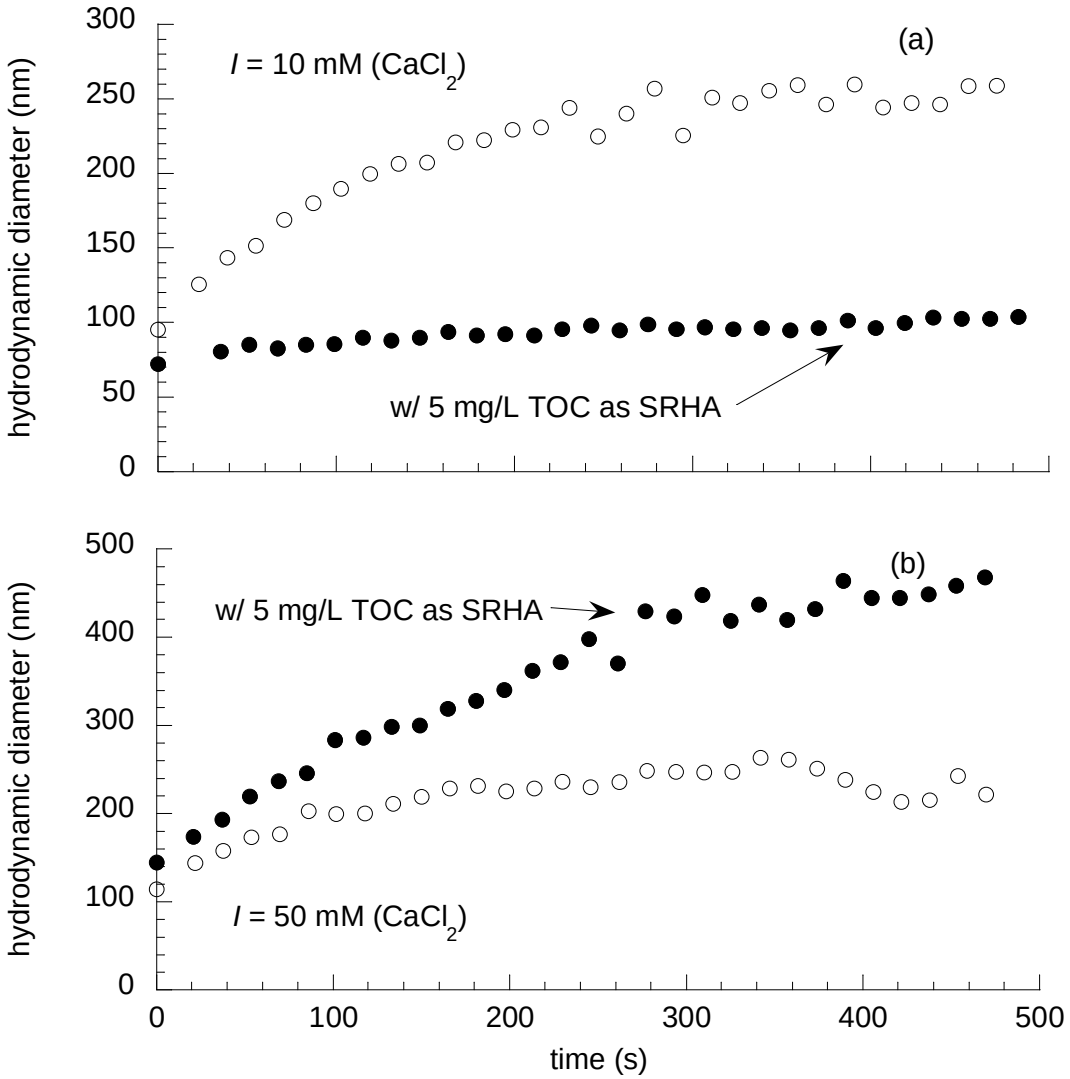

Figure A7. Time-resolved dynamic light scattering results of CIT-AuNPs suspended in I = 10 mM ($CaCl_2$) (a) and I = 50 mM ($CaCl_2$) (b) with and without 5 mg L^{-1} TOC added as SRHA. At lower ionic strength, the presence of SRHA stabilized the NPs; at elevated Ca^{+2} concentrations, aggregation was enhanced due to cation bridging effects.

References

1. Liu, X. O.; Atwater, M.; Wang, J. H.; Huo, Q., Extinction coefficient of gold nanoparticles with different sizes and different capping ligands. *Colloids and Surfaces B-Biointerfaces* **2007,** *58*, (1), 3-7.
2. Diegoli, S.; Manciulea, A. L.; Begum, S.; Jones, I. P.; Lead, J. R.; Preece, J. A., Interaction between manufactured gold nanoparticles and naturally occurring organic macromolecules. *Science of the Total Environment* **2008,** *402*, (1), 51-61.

Appendix B: Statistical Analysis of Zeta Potential Titrations

Hypothesis testing was performed to determine if there is a significant difference between samples with and without SRHA. Simplifying assumptions are made in order to perform t-tests on means at select pH values; 1.) zeta potential varies with pH and discreet samples with and without SRHA have slightly different pH values 2.) it is assumed that because data was collected in the same manner with and without SRHA, standard deviations are approximately the same and can be estimated by a pooled standard deviation.

A pooled standard deviation (s_{pooled}) is determined:

$$s_{pooled} = \sqrt{\frac{(n_1 - 1)s_1^2 + (n_2 - 1)s_2^2}{(n_1 - 1) + (n_2 - 1)}}$$

Where n_1 replicate analysis of sample 1 yield a mean of $\bar{x}_1$ with standard deviation s_1 and n_2 replicate analysis of sample 2 yield a mean of $\bar{x}_2$ with standard deviation s_2.

A test value of t is then given by:

$$t = \frac{\bar{x}_1 - \bar{x}_2}{s_{pooled}\sqrt{\frac{n_1 + n_2}{n_1 n_2}}}$$

The calculated t value is then compared with the critical value of t obtained from a t-table for 95% confidence level and $n_1 + n_2 - 2$ degrees of freedom. If the calculated (absolute) t value of is less than the critical t value then there is no difference between the means [1].

Table B.1 summarizes evaluations of discreet samples between NPs with and without SRHA. *t* tests conducted for the MPTMA-AuNPs and PVP-AuNPs revealed significant differences at low pH values, while at high pH (9 and 10) there was no significant difference in the means. As for the MEEE-AuNPs there was only a statistical

significance between means with and without SRHA at pH 10. The means of the intrinsic ζ of CIT- and TAN-AuNPs tended to be less negative without SRHA, with the exception of pH 6. The evaluations confirm the decreasing trend in surface charge of AuNPs in the presence of SRHA. Shown in Table B2. is a summary of the evaluations of the three ionic (MPTMA, CIT, TAN) NPs with SRHA, respectively. The analysis was conducted in pair-wise combinations of the three AuNPs at select pH values. The means between the samples had significant differences for the only three points: MPTMA+SRHA and CIT+SRHA (pH 3 and 6); CIT+SRHA and TAN+SRHA (pH 10). The rough statistical analysis confirms the observation that electrostatically stabilized AuNPs exhibited similar charge behavior as influenced by SRHA.

Future experiments should be designed to make more robust statistical comparisons. A major improvement could be achieved by conducting analyses with and without SRHA at the same pH. Additionally, evaluations could be performed at higher confidence levels for more compelling evidence of statistical significance.

Table B1. Statistical evaluation of zeta potential titrations of AuNPs with and without SRHA.

Sample Comparison	pH	n_1	n_2	s_{pooled}	t_{abs}	t_{crit}	Difference
MPTMA	3	10	10	7.39	24.43	2.101	
	6	7	10	9.91	13.42	2.131	
MPTMA+SRHA	9	10	9	22.77	1.73	2.11	None
	10	10	8	21.04	1.07	2.12	None
PVP	3	9	10	5.40	3.48	2.11	
	6	10	9	5.03	2.81	2.11	
PVP+SRHA	9	10	10	9.25	1.32	2.101	None
	10	10	9	4.68	1.41	2.11	None
MEEE	3	8	10	4.34	0.48	2.12	None
	6	10	10	10.93	0.97	2.101	None
MEEE+SRHA	9	9	10	6.05	1.51	2.11	None
	10	10	10	8.41	2.29	2.101	
CIT	3	10	10	4.52	2.90	2.101	
	6	10	7	5.87	1.57	2.131	None
CIT+SRHA	9	10	10	6.02	3.87	2.101	
	10	10	8	5.13	3.48	2.12	
TAN	3	10	10	4.34	8.35	2.101	
	6	10	10	8.63	1.99	2.101	None
TAN+SRHA	9	10	10	8.22	2.13	2.101	
	10	10	10	5.06	5.39	2.101	

Table B2. Statistical evaluation of zeta potential titrations of ionic functionalized AuNPs with SRHA.

Sample Comparison	pH	n_1	n_2	s_{pooled}	t_{abs}	t_{crit}	Difference
MPTMA+SRHA	3	10	10	5.62	2.19	2.101	
	6	10	7	6.25	2.48	2.131	
CIT+SRHA	9	9	10	7.85	0.55	2.11	None
	10	8	8	5.18	1.16	2.14	None
MPTMA+SRHA	3	10	10	6.16	0.65	2.101	None
	6	10	10	6.19	1.74	2.101	None
TAN+SRHA	9	9	10	7.66	1.28	2.11	None
	10	8	10	4.75	2.52	2.12	
CIT+SRHA	3	10	10	4.24	1.96	2.101	None
	6	7	10	3.69	1.56	2.131	None
TAN+SRHA	9	10	10	4.32	1.30	2.101	None
	10	8	10	3.07	1.84	2.12	None

References

1. Douglas A. Skoog, D.M.W., F. James Holler, and Stanley R. Crouch, Analytical Chemistry, An Introduction. 7 ed. 2000, New York: Saunders College Publishing.